Semi-blind joint symbols and multipath parameters estimation of MIMO systems using KRST/MKRSM coding

S V N Randriambelonoro, G Favier, Remy Boyer

Semi-blind joint symbols and multipath parameters estimation of MIMO systems using KRST/MKRSM coding

S. V. N. Randriambelonoro[a,b], G. Favier[b,*], R. Boyer[c]

[a] *Ecole Doctorale en Sciences et Techniques de l'Ingénierie et de l'Innovation Université d'Antananarivo, TASI Laboratory, Madagascar.*
[b] *Université Côte d'Azur, CNRS, Sophia Antipolis, I3S Laboratory, France.*
[c] *University of Lille-1, CRIStAL Laboratory, France.*

Abstract

In this paper, we propose a new MIMO communication system in a time-varying multipath environment, using a Khatri-Rao space-time (KRST) coding combined with a multiple Khatri-Rao product of symbol matrices (MKRSM). It is shown the signals received at the receiver form a tensor which satisfies a $(M+2)$-order nested PARAFAC model, where $(M-1)$ denotes the number of symbol matrices considered for MKRSM coding. Such a generalization of the nested PARAFAC model to $(M+N)$-order tensors is first studied from a general point of view, with the discussion of some parameter estimation methods depending on the a priori knowledge on the model. Then, a semi-blind receiver composed of three stages, is developed for jointly estimating the transmitted symbols and the multipath parameters. In the first stage, the transmitted symbols and a matrix unfolding of the effective channel including the fading coefficients and the steering matrices, are estimated using closed-form algorithms based on Khatri-Rao factorizations. In the second one, the channel estimation is refined by means of a simplified least-squares algorithm which takes the column orthonormality assumption on the coding matrix into account. In the third one, an alternating least-squares algorithm, combined with a rectification for the Vandermonde factors containing the spatial steering vectors at the transmitter and receiver sides, is applied to estimate the multipath parameters from the estimated channel. A complexity analysis is made for the receivers, and an expected Cramer-Rao bound related to channel estimation is established. Extensive

*Corresponding author
Email addresses: nokoloina@i3s.unice.fr (S. V. N. Randriambelonoro), favier@i3s.unice.fr (G. Favier), remy.boyer@univ-lille.fr (R. Boyer)

Monte Carlo simulation results show that the semi-blind receiver which combines the channel estimation refinement with the rectification technique exhibit very interesting performance.
Keywords: MIMO systems, Khatri-Rao space-time (KRST) coding, multiple Khatri-Rao product of symbol matrices (MKRSM), multiple Khatri-Rao factorization (MKRF) based decoding, generalized nested PARAFAC model, semi-blind receiver, rectification technique.

1. Introduction

As it is well known, multiple-input multiple-output (MIMO) wireless communication systems allow to increase channel capacity. However, to maximize capacity gains a perfect knowledge of the channel state is needed, hence the importance of channel estimation. Besides the space diversity brought by multi antenna arrays, space-time coding is used to increase the redundancy of transmitted information symbols, and so the diversity gain.

During the last two decades, wireless communication systems have been one of the main fields of application of high order tensor decompositions. A lot of works have proposed tensor-based MIMO communication systems, first for point to point systems and then for cooperative ones with relays. Most of systems are based on the PARAFAC model [1], or variants like constrained and nested PARAFAC models [2], [3], [4], [5], [6]. Overviews of such MIMO systems can be found in [7] and [8]. In the case of cooperative systems, new tensor models have been recently developed such as nested Tucker [9], coupled nested Tucker [10], and tensor train [11] ones.

High order tensors have been used for designing tensor codings like tensor space time (TST) and tensor space time frequency (TSTF) ones ([12], [13]) for CDMA and OFDM systems, respectively. An advantage of tensor coding is that multiple diversities can be simultaneously taken into account, like space, time, frequency and coding diversities. Recently, a new generalized Khatri-Rao coding has been proposed based on a multiple Khatri-Rao product of symbol matrices (MKRSM), in the context of MIMO relays systems [14].

A specificity of tensor-based communication systems lies in the possibility of joint semi-blind estimation of information symbols and channel. However, most of the systems do not take a multipath environment into account, and consequently the problem of jointly estimating propagation path loss coefficients with direction-of-departure (DoD) and direction-

of-arrival (DoA) angles is not addressed.

Generally speaking, the problem of angle estimation plays a fundamental role in array signal processing applications [15]. Two important fields of application concern bistatic MIMO radar whose antennas in transmit and receive arrays are closely spaced, also called colocated MIMO radar [16], and MIMO communication systems. Since the pioneering works [17] [18] of Schmidt (1986) and Roy and Kailath (1989) who introduced the popular subspace-based methods called MUSIC (multiple signal classification) and ESPRIT (estimation of signal parameters via rotational invariance technique), a lot of MUSIC-based and ESPRIT-based algorithms have been developed to solve the DoD and DoA estimation problem. In recent years, tensor-based methods have been proposed for joint DoD and DoA estimation in the context of bistatic MIMO radar [19], [20], [21], [22], [23], [24], [25], [26]. Several tensor-based angle estimation methods have also been developed for multipath MIMO wireless communication systems as in [27], [28], [29].

In the present paper, we propose a MIMO communication system in a time varying multipath environment, which combines a Khatri-Rao space-time (KRST) coding [30] with a MKRSM [14]. It is shown the received signals satisfy a new generalized nested PARAFAC model which is exploited to develop a semi-blind receiver for jointly estimating the information symbols, the channel and the multipath parameters. This receiver is composed of three stages. In the first one, a closed form algorithm based on a multiple Khatri-Rao factorization (MKRF) is used for jointly estimating the symbol matrices and a matrix unfolding of the third-order channel tensor. In the second one, the channel estimation is refined by means of a simplified least-squares algorithm which takes into account both the information symbols estimated in the first stage and the column orthonormality assumption on the coding matrix. This solution which combines the MKRF and LS algorithms for symbols and refined channel estimation, will be called the MKRF/LS receiver. In the third stage, the third-order PARAFAC model satisfied by the channel tensor is exploited in applying the alternating least squares (ALS) algorithm to jointly estimate the fading coefficients, DoD and DoA angles, using the channel estimated in the first or second stage. A rectification algorithm [31] is employed to improve the DoD and DoA angles estimation in taking into account the Vandermonde structure of the steering matrices. Indeed, in a noisy environment,

each column of the steering matrices estimated using the ALS scheme is only approximatively Vandermonde-structured. So, to enforce this structure, the RecALS method proposed in [31], is used. This approach is based on the mapping of a Vandermonde vector toward a rank-one Toeplitz matrix of which the non-zero eigenvalue is relied to the angular-frequency of the closest Vandermonde structured vector.

The main contributions of this paper can be summarized as follows:

- A new MIMO communication system combining KRST/MKRSM codings is proposed in a time varying multipath scenario, leading to a generalized nested PARAFAC model for the tensor of received signals.
- This new nested PARAFAC decomposition is studied from a general point of view, and some parameter estimation methods are discussed.
- Semi-blind MKRF/LS/ALS and MKRF/ALS receivers including a rectification method are developed, with removal of ambiguities inherent to MKRF and ALS algorithms.
- Parameters identifiability conditions are established, and the computational complexity of the proposed receivers is analyzed.
- An original expected Cramer-Rao bound (CRB) related to channel estimation using the MKRF algorithm is derived exploiting both a column-orthonormal assumption for the KRST coding matrix and QAM modulation for the information symbols.
- Extensive Monte Carlo simulation results show that the semi-blind receiver which combines the channel estimation refinement with the rectification technique exhibit very interesting performance.

The rest of this paper is organized as follows. Section 2 presents a new multipath MIMO communication system combining KRST coding with MKRSM. It is shown the received signals form a tensor which satisfies a generalized nested PARAFAC model. Uniqueness conditions for this model are given. In Section 3, this new nested-PARAFAC decomposition is studied for $(M + N)$-order tensors. Algorithms for parameter estimation are discussed according to the a priori knowledge on matrix factors. Section 4 is dedicated to the derivation

of two semi-blind receivers, called MKRF/ALS and MKRF/LS/ALS, assuming the coding matrix is known at the receiver. In Section 5, the removal of ambiguities is discussed, and the receivers complexity is anayzed. In Section 6, the expected CRB for channel estimation is derived. Section 7 presents extensive Monte Carlo simulation results to illustrate the performance of the proposed receivers, before concluding the paper in Section 8.

Notation: Scalars, vectors, matrices, and tensors of order higher than two are written using lower-case, boldface lower-case, bold face upper-case, and calligraphic letters (*e.g.*, a, $\mathbf{a}$, $\mathbf{A}$, and $\boldsymbol{\mathcal{A}}$, respectively). $\mathbf{A}^T, \mathbf{A}^*$, $\mathbf{A}^H$ and $\mathbf{A}^\dagger$ stand for transpose, complex conjugate, Hermitian transpose, and Moore-Penrose pseudo-inverse of $\mathbf{A}$. Outer, Kronecker, Khatri-Rao and Hadamard products are denoted by $\circ$, $\otimes$, $\diamond$ and $\odot$, respectively. $\mathbf{I}_R$ and $\boldsymbol{\mathcal{I}}_{R,N}$ denote the identity matrix of dimension $R \times R$ and the identity tensor of order N and dimension $R \times \cdots \times R$, whereas $\mathbf{A}_{i.}$ and $\mathbf{A}_{.j}$ represent the i-th row and the j-th column of $\mathbf{A} \in \mathbb{C}^{I \times J}$, and $\text{diag}(\lambda_1, \cdots, \lambda_N)$ is the diagonal matrix with the elements $\lambda_n, n \in \langle N \rangle$ on the diagonal, where $\langle N \rangle = \{1, \cdots, N\}$ denotes the set of the first N natural integers,

Hereafter, we recall some useful properties which will be used in the paper.

- For $\mathbf{A} \in \mathbb{C}^{I \times J}, \mathbf{B} \in \mathbb{C}^{K \times L}, \mathbf{C} \in \mathbb{C}^{J \times K}$, we have:

$$\text{vec}(\mathbf{ACB}) = (\mathbf{B}^T \otimes \mathbf{A})\text{vec}(\mathbf{C}) \in \mathbb{C}^{LI}. \tag{1}$$

- For $\mathbf{A} \in \mathbb{C}^{I \times J}$, $\mathbf{B} \in \mathbb{C}^{M \times N}$, $\mathbf{C} \in \mathbb{C}^{J \times K}$, and $\mathbf{D} \in \mathbb{C}^{N \times P}$, we have:

$$(\mathbf{A} \otimes \mathbf{B})(\mathbf{C} \otimes \mathbf{D}) = \mathbf{AC} \otimes \mathbf{BD} \in \mathbb{C}^{IM \times KP}. \tag{2}$$

- For $\mathbf{A} \in \mathbb{C}^{I \times K}, \mathbf{B} \in \mathbb{C}^{J \times K}, \mathbf{C} \in \mathbb{C}^{I \times L}$ and $\mathbf{D} \in \mathbb{C}^{J \times L}$, we have:

$$(\mathbf{A} \diamond \mathbf{B})^H(\mathbf{C} \diamond \mathbf{D}) = \mathbf{A}^H\mathbf{C} \odot \mathbf{B}^H\mathbf{D} \in \mathbb{C}^{K \times L}. \tag{3}$$

- Banachiewicz-Schur' formula for the inverse of a partitioned matrix:

$$\begin{bmatrix} \mathbf{A} & \mathbf{B} \\ \mathbf{C} & \mathbf{D} \end{bmatrix}^{-1} = \begin{bmatrix} \mathbf{A}^{-1} + \mathbf{A}^{-1}\mathbf{B}\mathbf{X}_\mathbf{A}^{-1}\mathbf{C}\mathbf{A}^{-1} & -\mathbf{A}^{-1}\mathbf{B}\mathbf{X}_\mathbf{A}^{-1} \\ -\mathbf{X}_\mathbf{A}^{-1}\mathbf{C}\mathbf{A}^{-1} & \mathbf{X}_\mathbf{A}^{-1} \end{bmatrix} \tag{4}$$

$$\mathbf{X}_\mathbf{A} = \mathbf{D} - \mathbf{C}\mathbf{A}^{-1}\mathbf{B}. \tag{5}$$

- If the matrices $\mathbf{A} \in \mathbb{C}^{I \times J}$ and $\mathbf{B} \in \mathbb{C}^{K \times L}$ are full column rank, we have:

$$(\mathbf{A} \otimes \mathbf{B})^{\dagger} = \mathbf{A}^{\dagger} \otimes \mathbf{B}^{\dagger}. \tag{6}$$

2. System model

We consider a MIMO communication system equipped with uniform linear arrays (ULAs) at both the transmitter and the receiver, composed of M_T and M_R antennas, respectively. The information symbols to be transmitted are coded using a KRST coding combined with a MKRSM of symbol matrices $\mathbf{S}^{(m)} = \left[\mathbf{s}_1^{(m)}, \cdots, \mathbf{s}_{M_T}^{(m)}\right] \in \mathbb{C}^{P_m \times M_T}$, with $m \in \{2, \cdots, M\}$. Defining $\prod_{m=2}^{M} P_m = P$, the coded signals can be written as:

$$\mathbf{U} = \mathbf{C} \diamond \mathbf{S}^{(2)} \diamond \cdots \diamond \mathbf{S}^{(M)} \in \mathbb{C}^{KP \times M_T}, \tag{7}$$

where $\mathbf{C} \in \mathbb{C}^{K \times M_T}$ is the KRST coding matrix. Each symbol matrix $\mathbf{S}^{(m)}$ contains P_m data streams composed of M_T symbols each. Defining $\mathbf{S} \triangleq \diamond_{m=2}^{M} \mathbf{S}^{(m)}$, the coded signals matrix $\mathbf{U}$ can be rewritten as:

$$\mathbf{U} = \mathbf{C} \diamond \mathbf{S}. \tag{8}$$

The coded signals transmitted by the m_T-th transmit antenna are given by:

$$u_{k,p_2 \cdots, p_M, m_T} = c_{k,m_T} \prod_{m=2}^{M} s_{p_m,m_T}^{(m)}. \tag{9}$$

The transmission is composed of T_s blocks, the coded signals (9) being transmitted during each time-block $t_s \in \langle T_s \rangle$. We assume that there exists L paths between the transmit and receive arrays, characterized by the DoD and DoA angles (φ_l, θ_l), with $l \in \langle L \rangle$, and fading coefficients $w_{t_s,l}$ depending on the transmission block t_s.

Let us define the steering matrices $\mathbf{B}^{(T)}$ at the transmitter and $\mathbf{B}^{(R)}$ at the receiver as:

$$\mathbf{B}^{(T)} = [\mathbf{b}^{(T)}(\varphi_1), \cdots, \mathbf{b}^{(T)}(\varphi_L)] \in \mathbb{C}^{M_T \times L} \tag{10}$$

$$\mathbf{B}^{(R)} = [\mathbf{b}^{(R)}(\theta_1), \cdots, \mathbf{b}^{(R)}(\theta_L)] \in \mathbb{C}^{M_R \times L} \tag{11}$$

with ($i^2 = -1$):

$$\mathbf{b}^{(T)}(\varphi_l) = [1, e^{-i\pi sin(\varphi_l)}, \cdots, e^{-i\pi(M_T-1)sin(\varphi_l)}]^T \in \mathbb{C}^{M_T} \tag{12}$$

$$\mathbf{b}^{(R)}(\theta_l) = [1, e^{-i\pi sin(\theta_l)}, \cdots, e^{-i\pi(M_R-1)sin(\theta_l)}]^T \in \mathbb{C}^{M_R} \tag{13}$$

and the matrix $\mathbf{W}$ containing the random complex time varying fading coefficients of the L paths during T_s transmission blocks:

$$\mathbf{W} = \begin{bmatrix} \mathbf{w}_1^T \\ \vdots \\ \mathbf{w}_{T_s}^T \end{bmatrix} \in \mathbb{C}^{T_s \times L} \tag{14}$$

with $\mathbf{w}_{t_s}^T = [w_{t_s,1}, \cdots, w_{t_s,L}], t_s \in \langle T_s \rangle$. Note that the DoD and DoA angles (φ_l, θ_l), with $l \in \langle L \rangle$, are assumed constant during the T_s transmission blocks, whereas the fading coefficients vary at each transmission block.

The coded signals (9) transmitted by the M_T transmit antennas through the l-th path are transformed as:

$$z_{k,p_2,\cdots,p_M,l} = \sum_{m_T=1}^{M_T} u_{k,p_2,\cdots,p_M,m_T} b_{m_T,l}^{(T)} = \sum_{m_T=1}^{M_T} c_{k,m_T} \prod_{m=2}^{M} s_{p_m,m_T}^{(m)} b_{m_T,l}^{(T)}. \tag{15}$$

This $(M+1)$-order tensor $\boldsymbol{\mathcal{Z}} \in \mathbb{C}^{K \times P_2 \times \cdots \times P_M \times L}$ can be interpreted as the tensor of the signals transmitted by the transmit array, after coding. It satisfies the rank-M_T PARAFAC model $[\![\mathbf{C}, \mathbf{S}^{(2)}, \cdots, \mathbf{S}^{(M)}, \mathbf{B}^{(T)}; M_T]\!]$.

After transmission through the L paths, the signals received at the m_R-th receive antenna, during the t_s time block, form a $(M+2)$-order tensor $\boldsymbol{\mathcal{X}}$ of dimension $K \times P_2 \times \cdots \times P_M \times M_R \times T_s$, given by:

$$x_{k,p_2,\cdots,p_M,m_R,t_s} = \sum_{l=1}^{L} z_{k,p_2,\cdots,p_M,l} b_{m_R,l}^{(R)} w_{t_s,l}. \tag{16}$$

Replacing $z_{k,p_2,\cdots,p_M,l}$ by its expression (15) in the above equation, we obtain:

$$x_{k,p_2,\cdots,p_M,m_R,t_s} = \sum_{m_T=1}^{M_T} \sum_{l=1}^{L} c_{k,m_T} \Big(\prod_{m=2}^{M} s_{p_m,m_T}^{(m)} \Big) b_{m_R,l}^{(R)} b_{m_T,l}^{(T)} w_{t_s,l} \tag{17}$$

$$= \sum_{m_T=1}^{M_T} c_{k,m_T} \prod_{m=2}^{M} s_{p_m,m_T}^{(m)} h_{m_R,t_s,m_T} \tag{18}$$

where:

$$h_{m_R,t_s,m_T} = \sum_{l=1}^{L} b^{(R)}_{m_R,l} w_{t_s,l} b^{(T)}_{m_T,l} \tag{19}$$

is an entry of the effective channel tensor $\boldsymbol{\mathcal{H}} \in \mathbb{C}^{M_R \times T_s \times M_T}$, between the m_T-th transmit antenna and the m_R-th receive antenna, during the time block t_s, along the L paths. From Eq. (19), we can conclude that this third-order tensor satisfies the rank-L PARAFAC model $[\![\mathbf{B}^{(R)}, \mathbf{W}, \mathbf{B}^{(T)}; L]\!]$. The t_s-th slice along mode-2 of this tensor is given by:

$$\mathbf{H}_{M_R \times M_T}(t_s) = \mathbf{B}^{(R)} \mathbf{D}_{t_s}(\mathbf{W}) \left[\mathbf{B}^{(T)}\right]^T \in \mathbb{C}^{M_R \times M_T} \tag{20}$$

where $\mathbf{D}_{t_s}(\mathbf{W})$ denotes the diagonal matrix whose diagonal elements are the components of the row t_s of $\mathbf{W}$. From Eqs. (15) and (19), we can conclude that these PARAFAC models share a common factor $\mathbf{B}^{(T)}$, and Eq. (17) corresponds to the nesting of these two PARAFAC models. Such a model of the $(M+2)$-order tensor $\boldsymbol{\mathcal{X}}$ will be called a generalized nested PARAFAC decomposition. This new tensor decomposition is studied in more detail in the next section before deriving semi-blind receivers for the proposed MIMO system.

Fig. 1 represents the block diagram of the MIMO system. The definitions of the design parameters and of the system matrices and tensors are summarized in Tables 1 and 2, respectively.

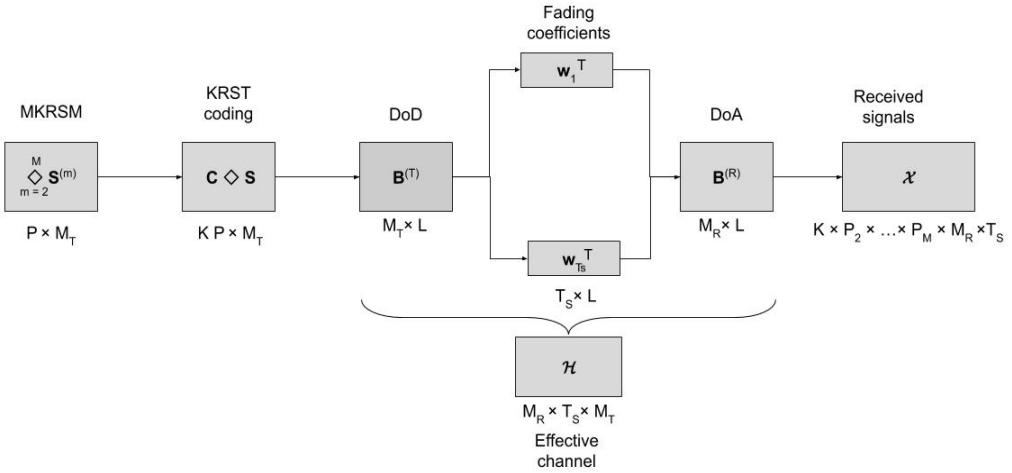

Figure 1: Block diagram of the MIMO system

Uniqueness conditions are presented in the following lemma.

Lemma: Applying the Kruskal's condition [32], we can deduce that the generalized nested

Table 1: Design parameters

Design parameters	Definitions
M	number of symbol matrices
P_m	number of data streams for the m-th symbol matrix
P	product of all P_m for $m \in \{2, \cdots, M\}$
M_T	number of transmit antennas
M_R	number of receive antennas
T_s	number of transmission blocks
L	number of multipaths
K	coding length
φ	DoD angle
θ	DoA angle

Table 2: System matrices and tensors

Matrices	Definitions	Dimensions
$\mathbf{C}$	coding matrix	$K \times M_T$
$\mathbf{S}^{(m)}$	m-th symbol matrix	$P_m \times M_T$
$\mathbf{B}^{(T)}$	steering matrix at the transmitter	$M_T \times L$
$\mathbf{B}^{(R)}$	steering matrix at the receiver	$M_R \times L$
$\mathbf{W}$	time varying fading matrix	$T_s \times L$
Tensors	Definitions	Dimensions
$\boldsymbol{\mathcal{X}}$	received signals tensor	$K \times P_2 \times \cdots \times P_M \times M_R \times T_s$
$\boldsymbol{\mathcal{H}}$	effective channel tensor	$M_R \times T_s \times M_T$
$\boldsymbol{\mathcal{Z}}$	coded transmitted signals tensor	$K \times P_2 \times \cdots \times P_M \times M_T$

PARAFAC model of the proposed MIMO system is essentially unique if the following con-

ditions relative to the PARAFAC models (15) and (19) are satisfied:

$$k_{\mathbf{C}} + \sum_{m=2}^{M} k_{\mathbf{S}^{(m)}} + k_{\mathbf{B}^{(T)}} \geq 2M_T + M \tag{21}$$

$$k_{\mathbf{B}^{(R)}} + k_{\mathbf{W}} + k_{\mathbf{B}^{(T)}} \geq 2L + 2 \tag{22}$$

where $k_{\mathbf{A}}$ denotes the k-rank of $\mathbf{A}$, i.e., the largest integer k such that all subsets of k columns of $\mathbf{A}$ are linearly independent. Essential uniqueness means that the matrix factors of the nested PARAFAC model are unique up to column permutation and scaling ambiguities. Under the assumption that all the factor matrices are full rank, the previous conditions become:

$$\min(K, M_T) + \sum_{m=2}^{M} \min(I_m, M_T) + \min(L, M_T) \geq 2M_T + 2 \tag{23}$$

$$\min(M_R, L) + \min(T_s, L) + \min(M_T, L) \geq 2L + 2. \tag{24}$$

3. Generalized nested PARAFAC decomposition

In this section, we study a generalization of the nested PARAFAC model, introduced in [3] for a fourth-order tensor, to $(M+N)$-order tensors $\boldsymbol{\mathcal{X}} \in \mathbb{C}^{I_1 \times \cdots \times I_M \times J_1 \times \cdots \times J_N}$. Such a model is written in scalar form as:

$$x_{i_1,\cdots,i_M,j_1,\cdots,j_N} = \sum_{p=1}^{P} \sum_{q=1}^{Q} \Big(\prod_{m=1}^{M} a_{i_m,p}^{(m)} \Big) g_{p,q} \Big(\prod_{n=1}^{N} b_{j_n,q}^{(n)} \Big) \tag{25}$$

where $\mathbf{A}^{(m)} \in \mathbb{C}^{I_m \times P}$ and $\mathbf{B}^{(n)} \in \mathbb{C}^{J_n \times Q}$. It can be viewed as two nested-PARAFAC models sharing a common factor matrix $\mathbf{G} \in \mathbb{C}^{P \times Q}$. These PARAFAC models are associated with two tensors $\boldsymbol{\mathcal{Z}} \in \mathbb{C}^{I_1 \times \cdots \times I_M \times Q}$ and $\boldsymbol{\mathcal{H}} \in \mathbb{C}^{J_1 \times \cdots \times J_N \times P}$, of respective orders $(M+1)$ and $(N+1)$, and ranks P and Q, such as :

$$z_{i_1,\cdots,i_M,q} = \sum_{p=1}^{P} \Big(\prod_{m=1}^{M} a_{i_m,p}^{(m)} \Big) g_{p,q} \tag{26}$$

$$h_{j_1,\cdots,j_N,p} = \sum_{q=1}^{Q} \Big(\prod_{n=1}^{N} b_{j_n,q}^{(n)} \Big) g_{p,q}. \tag{27}$$

Using mode-n products, these PARAFAC models that will be called left PARAFAC (LP) and right PARAFAC (RP) models of the tensors $\boldsymbol{\mathcal{Z}}$ and $\boldsymbol{\mathcal{Y}}$, can also be written as:

$$\boldsymbol{\mathcal{Z}} = \boldsymbol{\mathcal{I}}_{M+1,P} \times_{m=1}^{M} \mathbf{A}^{(m)} \times_{M+1} \mathbf{G}^T \tag{28}$$

$$\boldsymbol{\mathcal{Y}} = \boldsymbol{\mathcal{I}}_{N+1,Q} \times_{n=1}^{N} \mathbf{B}^{(n)} \times_{N+1} \mathbf{G}. \tag{29}$$

They are concisely written as:

$$[\![\mathbf{A}^{(1)}, \cdots, \mathbf{A}^{(M)}, \mathbf{G}^T; P]\!] \text{ and } [\![\mathbf{B}^{(1)}, \cdots, \mathbf{B}^{(N)}, \mathbf{G}; Q]\!]. \tag{30}$$

This nested PARAFAC model is illustrated by means of Fig. 2.

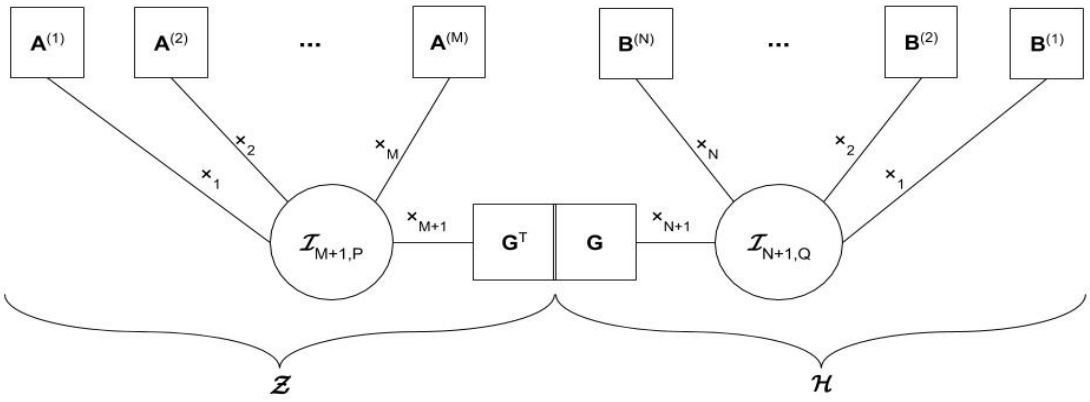

Figure 2: Generalized nested PARAFAC model

Comparing (17) with (25), we conclude that the received signals tensor $\boldsymbol{\mathcal{X}}$ satisfies a generalized nested PARAFAC model, with the following correspondences:

$$(I_1, I_2, \cdots, I_M, J_1, J_2, P, Q) \Leftrightarrow (K, P_2, \cdots, P_M, M_R, T_s, M_T, L)$$

$$(\mathbf{A}^{(1)}, \mathbf{A}^{(2)}, \cdots, \mathbf{A}^{(M)}, \mathbf{B}^{(1)}, \mathbf{B}^{(2)}, \mathbf{G}) \Leftrightarrow (\mathbf{C}, \mathbf{S}^{(2)}, \cdots, \mathbf{S}^{(M)}, \mathbf{B}^{(R)}, \mathbf{W}, \mathbf{B}^{(T)}).$$

The LP and RP models, of respective orders $M+1$ and 3, correspond to Eq. (15) and (19), with the factor matrices $(\mathbf{C}, \mathbf{S}^{(2)}, \cdots, \mathbf{S}^{(M)}, [\mathbf{B}^{(T)}]^T)$ and $(\mathbf{B}^{(R)}, \mathbf{W}, \mathbf{B}^{(T)})$, respectively, and with $\mathbf{B}^{(T)} \in \mathbb{C}^{M_T \times L}$ as common matrix factor.

Applying the Kruskal's uniqueness condition [32], we can conclude that these PARAFAC models are essentially unique if the sufficient (but not necessary) conditions are satisfied:

$$\sum_{m=1}^{M} k_{\mathbf{A}^{(m)}} + k_{\mathbf{G}^T} \geq 2P + M \ ; \ \sum_{n=1}^{N} k_{\mathbf{B}^{(n)}} + k_{\mathbf{G}} \geq 2Q + N. \tag{31}$$

Using definitions (26) and (27) in Eq. (25), the tensor $\boldsymbol{\mathcal{X}}$ can be rewritten in the following two scalar forms:

$$x_{i_1,\cdots,i_M,j_1,\cdots,j_N} = \sum_{p=1}^{P} \prod_{m=1}^{M} a^{(m)}_{i_m,p} h_{j_1,\cdots,j_N,p} \tag{32}$$

$$= \sum_{q=1}^{Q} \prod_{n=1}^{N} b^{(n)}_{j_n,q} z_{i_1,\cdots,i_M,q}\,. \tag{33}$$

Defining the matrix unfoldings $\mathbf{Z}_{\prod_{m=1}^{M} I_m \times Q}$ and $\mathbf{H}_{\prod_{n=1}^{N} J_n \times P}$ of tensors $\boldsymbol{\mathcal{Z}}$ and $\boldsymbol{\mathcal{H}}$, one can associate two PARAFAC models $\left\{\left\{\mathbf{A}^{(1)},\cdots,\mathbf{A}^{(M)},\mathbf{H}_{\prod_{n=1}^{N} J_n \times P};P\right\}\right\}$ and $\left\{\left\{\mathbf{B}^{(1)},\cdots,\mathbf{B}^{(N)},\right.\right.$ $\left.\left.\mathbf{Z}_{\prod_{m=1}^{M} I_m \times Q};Q\right\}\right\}$ to the contracted forms $\boldsymbol{\mathcal{X}}_{I_1\times\cdots\times I_M\times \prod_{n=1}^{N} J_n}$ and $\boldsymbol{\mathcal{X}}_{\prod_{m=1}^{M} I_m\times J_1\times\cdots\times J_N}$ of tensor $\boldsymbol{\mathcal{X}}$ resulting from the combination of modes $(j_1,\cdots,j_N)$ on one hand, and $(i_1,\cdots,i_M)$ on the other hand. These two PARAFAC models will be called left internal PARAFAC (LIP) and right internal PARAFAC (RIP) models of the tensor $\boldsymbol{\mathcal{X}}$, respectively.

In order to derive parameter estimation algorithms, we present some matrix unfoldings deduced from the PARAFAC models (32) and (33):

$$\mathbf{X}_{\prod_{\substack{m=1\\m\neq i}}^{M} I_m \ \prod_{n=1}^{N} J_n \times I_i} = \left(\diamond_{\substack{m=1\\m\neq i}}^{M} \mathbf{A}^{(m)} \diamond \mathbf{H}_{\prod_{n=1}^{N} J_n \times P}\right)\left(\mathbf{A}^{(i)}\right)^T, \ \ i \in \langle M\rangle \tag{34}$$

$$\mathbf{X}_{\prod_{m=1}^{M} I_m \times \prod_{n=1}^{N} J_n} = \left(\diamond_{m=1}^{M} \mathbf{A}^{(m)}\right)\mathbf{H}_{P\times \prod_{n=1}^{N} J_n} \tag{35}$$

and

$$\mathbf{X}_{\prod_{\substack{n=1\\n\neq j}}^{N} J_n \ \prod_{m=1}^{M} I_m \times J_j} = \left(\diamond_{\substack{n=1\\n\neq j}}^{N} \mathbf{B}^{(n)} \diamond \mathbf{Z}_{\prod_{m=1}^{M} I_m \times Q}\right)\left(\mathbf{B}^{(j)}\right)^T, \ \ j \in \langle N\rangle. \tag{36}$$

$$\mathbf{X}_{\prod_{n=1}^{N} J_n \times \prod_{m=1}^{M} I_m} = \left(\diamond_{n=1}^{N} \mathbf{B}^{(n)}\right)\mathbf{Z}_{Q\times \prod_{m=1}^{M} I_m}. \tag{37}$$

Moreover, for the PARAFAC models (26) and (27) of tensors $\boldsymbol{\mathcal{Z}}$ and $\boldsymbol{\mathcal{H}}$, we have:

$$\mathbf{Z}_{\prod_{m=1}^{M} I_m \times Q} = (\diamond_{m=1}^{M} \mathbf{A}^{(m)})\mathbf{G} \in \mathbb{C}^{\prod_{m=1}^{M} I_m \times Q} \tag{38}$$

$$\mathbf{H}_{\prod_{n=1}^{N} J_n \times P} = (\diamond_{n=1}^{N} \mathbf{B}^{(n)})\mathbf{G}^T \in \mathbb{C}^{\prod_{n=1}^{N} J_n \times P}. \tag{39}$$

Note that, from Eq. (35) and (39), we can deduce another matrix unfolding of $\boldsymbol{\mathcal{X}}$:

$$\mathbf{X}_{\prod_{m=1}^{M} I_m \times \prod_{n=1}^{N} J_n} = (\diamond_{m=1}^{M} \mathbf{A}^{(m)})\, \mathbf{G}\, (\diamond_{n=1}^{N} \mathbf{B}^{(n)})^T. \tag{40}$$

We now discuss the problem of parameter estimation for the tensor model (25), considering three cases depending on the a priori knowledge on the factor matrices: i) no a priori knowledge; ii) only one known factor ($\mathbf{A}^{(1)}$ for the LP model or $\mathbf{B}^{(1)}$ for the RP model) as it is the case for the MIMO system proposed in the previous section; iii) two known factors ($\mathbf{A}^{(1)}$ and $\mathbf{B}^{(1)}$ for instance).

- Case 1: If no factor matrix is a priori known, the parameter estimation problem can be solved in three consecutive stages as follows:
  - Application of the ALS algorithm for estimating the factor matrices $\left(\mathbf{A}^{(1)}, \cdots, \mathbf{A}^{(M)}, \mathbf{H}_{\prod_{n=1}^{N} J_n \times P}\right)$ of the LIP model using the unfoldings (34)-(35) of $\boldsymbol{\mathcal{X}}$.
  - Reconstruction of tensor $\boldsymbol{\mathcal{H}}$.
  - Estimation of the factors $\left(\mathbf{B}^{(1)}, \cdots, \mathbf{B}^{(N)}, \mathbf{G}\right)$ of model (39) by means of the ALS algorithm applied to the reconstructed channel tensor $\boldsymbol{\mathcal{H}}$.

  A symmetric procedure can be used beginning with the estimation of the parameters of the RIP model using the unfoldings (36)-(37), then reconstructing tensor $\boldsymbol{\mathcal{Z}}$, and finally, estimating the parameters of the PARAFAC model (38).

  The above described estimation procedures do not allow eliminating the permutation and scalar ambiguities. The knowledge of one factor matrix in the LP and RP models is needed to eliminate the permutation ambiguities, which corresponds to the next case. We will see later that the removal of scalar ambiguities needs the knowledge of one row of some matrix factors.

- Case 2: Assuming that the factor matrix $\mathbf{A}^{(1)}$ is a priori known and full column rank, which implies $I_1 \geq P$, the parameter estimation problem can be solved in four consecutive stages:

  - Application of the LS algorithm to estimate the MKR product (MKRP) from Eq. (34) for $i = 1$:

$$\mathbf{A}^{(2)} \diamond \cdots \diamond \mathbf{A}^{(M)} \diamond \mathbf{H}_{\prod_{n=1}^{N} J_n \times P} = \mathbf{X}_{\prod_{m=2}^{M} I_m \prod_{n=1}^{N} J_n \times I_1} \left[(\mathbf{A}^{(1)})^T\right]^{\dagger}. \tag{41}$$

  - Use of the MKRF algorithm, described in Appendix B, to estimate $\left(\mathbf{A}^{(2)}, \cdots, \mathbf{A}^{(M)}, \mathbf{H}_{\prod_{n=1}^{N} J_n \times P}\right)$.
  - Reconstruction of tensor $\boldsymbol{\mathcal{H}}$.
  - Application of the ALS algorithm for estimating the matrices $\left(\mathbf{B}^{(1)}, \cdots, \mathbf{B}^{(N)}, \mathbf{G}\right)$ of the PARAFAC model (39) of $\boldsymbol{\mathcal{H}}$.

  By comparing with the Case 1, we conclude that the estimation algorithms differ by stage 1, the iterative ALS algorithm being replaced by the closed-form method based on the MKRF algorithm.

  In a symmetric way, if $\mathbf{B}^{(1)}$ is a priori known and full column rank, which implies $J_1 \geq Q$, a similar estimation procedure can be employed, beginning with the LS estimation of the MKRP from Eq. (36) for $j = 1$:

$$(\mathbf{B}^{(2)} \diamond \cdots \diamond \mathbf{B}^{(N)} \diamond \mathbf{Z}_{\prod_{m=1}^{M} I_m \times Q}) = \mathbf{X}_{\prod_{n=2}^{N} J_n \prod_{m=1}^{M} I_m \times J_1} \left[(\mathbf{B}^{(1)})^T\right]^{\dagger}, \tag{42}$$

  followed by the estimation of $\left(\mathbf{B}^{(2)}, \cdots, \mathbf{B}^{(N)}, \mathbf{Z}_{\prod_{m=1}^{M} I_m \times Q}\right)$ using the MKRF algorithm. Then, after reconstructing the tensor $\boldsymbol{\mathcal{Z}}$, the parameters $\left(\mathbf{A}^{(1)}, \cdots, \mathbf{A}^{(M)}, \mathbf{G}\right)$ of the PARAFAC model (38) are estimated by means of the ALS algorithm.

- Case 3: If two matrix factors are known ($\mathbf{A}^{(1)}$ and $\mathbf{B}^{(1)}$, for instance), we can combine both algorithms of Case 2, to estimate in a parallel way the factors $\left(\mathbf{A}^{(2)}, \cdots, \mathbf{A}^{(M)}, \mathbf{H}_{\prod_{n=1}^{N} J_n \times P}\right)$ and $\left(\mathbf{B}^{(2)}, \cdots, \mathbf{B}^{(N)}, \mathbf{Z}_{\prod_{m=1}^{M} I_m \times Q}\right)$ using the MKRF algorithm.

Exploiting the matrix unfolding (40) of $\boldsymbol{\mathcal{X}}$ gives the following LS estimate of the matrix factor $\mathbf{G}$:

$$\hat{\mathbf{G}} = (\diamond_{m=1}^{M} \hat{\mathbf{A}}^{(m)})^{\dagger} \mathbf{X}_{\prod_{m=1}^{M} I_m \times \prod_{n=1}^{N} J_n} [(\diamond_{n=1}^{N} \hat{\mathbf{B}}^{(n)})^T]^{\dagger}. \tag{43}$$

4. MKRF/ALS and MKRF/LS/ALS based receivers

In this section, we assume that the KRST coding matrix $\mathbf{C}$ is known at the receiver, which corresponds to Case 2 among the three situations discussed in Section 3 for solving the parameter estimation problem. In consequence, the proposed receiver is composed of the following stages: first, the MKRF algorithm is used to estimate the symbol matrices $\mathbf{S}^{(m)}, m \in \{2, \cdots, M\}$, and the matrix unfolding $\mathbf{H}_{T_s M_R \times M_T}$ of the channel tensor. Then, after reshaping the channel tensor $\boldsymbol{\mathcal{H}}$, the ALS algorithm is applied to estimate the three matrix factors of the channel by exploiting the PARAFAC model (19) of $\boldsymbol{\mathcal{H}}$.

From the LIP model (18), we deduce the following tall matrix unfolding of the received signals tensor $\boldsymbol{\mathcal{X}}$:

$$\mathbf{X}_{P T_s M_R \times K} = \left(\mathbf{S}^{(2)} \diamond \cdots \diamond \mathbf{S}^{(M)} \diamond \mathbf{H}_{T_s M_R \times M_T} \right) \mathbf{C}^T. \tag{44}$$

Let us assume that the coding matrix $\mathbf{C} \in \mathbb{C}^{K \times M_T}$ is column orthonormal, chosen as a truncated Fourier matrix such that:

$$c_{k,m_T} = \frac{1}{\sqrt{K}} \, \omega^{(k-1)\ (m_T-1)}, \ k \in \langle K \rangle \, , \, m_T \in \langle M_T \rangle \tag{45}$$

where $\omega = \mathrm{e}^{-2i\pi/K}$ and $i^2 = -1$. The right inverse of $\mathbf{C}^T$ then simplifies as: $(\mathbf{C}^T)^{\dagger} = \mathbf{C}^*(\mathbf{C}^T\mathbf{C}^*)^{-1} = \mathbf{C}^*$, so that the LS estimate of the multiple Khatri-Rao product (MKRP) can be calculated as:

$$\mathbf{S} \diamond \mathbf{H}_{T_s M_R \times M_T} = \mathbf{X}_{P T_s M_R \times K} \mathbf{C}^* \tag{46}$$

where $\mathbf{S} \triangleq \mathbf{S}^{(2)} \diamond \cdots \diamond \mathbf{S}^{(M)}$. Application of the MKRF algorithm described in Appendix B allows to estimate the symbol matrices and the matrix unfolding $\mathbf{H}_{T_s M_R \times M_T}$ of $\boldsymbol{\mathcal{H}}$.

For the multipath parameters estimation, we exploit the PARAFAC model (19) of the

channel tensor of which matrix unfoldings are given by:

$$\mathbf{H}_{M_R \times T_s M_T} = \mathbf{B}^{(R)} (\mathbf{W} \diamond \mathbf{B}^{(T)})^T \tag{47}$$

$$\mathbf{H}_{M_T \times T_s M_R} = \mathbf{B}^{(T)} (\mathbf{W} \diamond \mathbf{B}^{(R)})^T \tag{48}$$

$$\mathbf{H}_{T_s \times M_R M_T} = \mathbf{W} (\mathbf{B}^{(R)} \diamond \mathbf{B}^{(T)})^T. \tag{49}$$

Application of the ALS algorithm leads to an alternate LS estimation of $(\mathbf{B}^{(R)}, \mathbf{B}^{(T)}, \mathbf{W})$, by means of the following equations, where it denotes the iteration number:

$$\hat{\mathbf{B}}^{(R)}_{it+1} = \hat{\mathbf{H}}_{M_R \times T_s M_T} \left[(\hat{\mathbf{W}}_{it} \diamond \hat{\mathbf{B}}^{(T)}_{it})^T \right]^\dagger \tag{50}$$

$$\hat{\mathbf{B}}^{(T)}_{it+1} = \hat{\mathbf{H}}_{M_T \times T_s M_R} \left[(\hat{\mathbf{W}}_{it} \diamond \hat{\mathbf{B}}^{(R)}_{it+1})^T \right]^\dagger \tag{51}$$

$$\hat{\mathbf{W}}_{it+1} = \hat{\mathbf{H}}_{T_s \times M_R M_T} \left[(\hat{\mathbf{B}}^{(R)}_{it+1} \diamond \hat{\mathbf{B}}^{(T)}_{it+1})^T \right]^\dagger. \tag{52}$$

Remark 1. At this stage, two semi-blind receivers can be proposed depending on the channel estimate used in the above Eqs. (50)-(52) of the ALS algorithm. The first one uses the channel estimate delivered by the MKRF algorithm applied to Eq. (46). It will be called the MKRF/LS receiver. The second one uses a refined estimation of the channel in the vectorized form $\hat{\mathbf{h}} = \text{vec}(\hat{\mathbf{H}}_{M_T \times T_s M_R})$, given by Eq. (84), and derived in Remark 4. The corresponding receiver, called MKRF/LS/ALS, is composed of three stages: MKRF for symbols and channel estimation; LS for a refinement of channel estimation; ALS for multipath parameters estimation. As it will be illustrated by simulation results, this second receiver allows to significantly improve the system performance, at the price of an additional cost that is negligible comparatively to the ALS one.

Necessary conditions for uniqueness of the right inverses in Eqs. (50)-(52) are such as the matrices to be inverted must have a number of columns greater than or equal to the number of rows, which implies the following necessary condition for identifiability of the channel factors: $\min(T_s M_T, T_s M_R, M_R M_T) \geq L$.

5. Ambiguity removal and receivers complexity analysis

Each stage of the receiver is characterized by ambiguities that are now described. In the first stage which consists in the MKRF algorithm, the ambiguities result from the KRP (46).

Recall that in the case of a single KRP of two vectors, there exists a scalar ambiguity which can be removed using the knowledge of one component of one of the two vectors.

Defining the estimate $\hat{\mathbf{S}} = \overset{M}{\underset{m=2}{\diamond}} \hat{\mathbf{S}}^{(m)}$ and assuming that the first row of each symbol matrix is composed of 1's, the equations for removing the ambiguities are given by:

$$\hat{\hat{\mathbf{S}}} = \hat{\mathbf{S}}\,\mathbf{\Delta}_S \;\text{ with }\; \mathbf{\Delta}_S = \left[\text{diag}(\hat{\mathbf{S}}_{1.})\right]^{-1} \tag{53}$$

and

$$\hat{\hat{\mathbf{H}}}_{T_s M_R \times M_T} = \hat{\mathbf{H}}_{T_s M_R \times M_T}\,\mathbf{\Delta}_H \;\text{ with }\; \mathbf{\Delta}_S \mathbf{\Delta}_H = \mathbf{I}_{M_T}. \tag{54}$$

In consequence, for the MKRF algorithm based on Eq. (46), the MKRP $\mathbf{S}^{(2)} \diamond \cdots \diamond \mathbf{S}^{(M)}$ being equivalent to $M-2$ KRPs of M_T vectors, the a priori knowledge of the first row of the symbol matrices $\mathbf{S}^{(m)} \in \mathbf{C}^{P_m \times M_T}, m \in \{2, \cdots, M\}$ is sufficient to remove the ambiguities in the estimated symbol matrices, so that:

$$\hat{\hat{\mathbf{S}}}^{(m)} = \hat{\mathbf{S}}^{(m)}\,\mathbf{\Delta}_S^{(m)} \;\text{ with }\; \mathbf{\Delta}_S^{(m)} = \left[\text{diag}(\hat{\mathbf{S}}_{1.}^{(m)})\right]^{-1},\; m \in \{2, \cdots, M\}. \tag{55}$$

After ambiguity suppression, the estimated symbols are projected onto the alphabet, which gives the final estimated symbol matrices denoted $\hat{\hat{\hat{\mathbf{S}}}}^{(m)}$, with $m \in \{2, \cdots, M\}$.

With the ALS algorithm based on Eqs. (50)-(52), the ambiguities are defined in terms of a permutation matrix and three diagonal scaling matrices which can be removed using the following equations:

$$\hat{\hat{\mathbf{B}}}^{(R)} = \hat{\mathbf{B}}^{(R)}\mathbf{\Delta}_{B^{(R)}} \;,\; \hat{\hat{\mathbf{B}}}^{(T)} = \hat{\mathbf{B}}^{(T)}\mathbf{\Delta}_{B^{(T)}} \;,\; \hat{\hat{\mathbf{W}}} = \hat{\mathbf{W}}\mathbf{\Delta}_W, \tag{56}$$

with $\mathbf{\Delta}_{B^{(R)}}\mathbf{\Delta}_{B^{(T)}}\mathbf{\Delta}_W = \mathbf{I}_L$. Exploiting the Vandermonde structure of the receive and transmit steering matrices $\mathbf{B}^{(R)}$ and $\mathbf{B}^{(T)}$, characterized by a first row composed of 1's, we deduce the following scaling ambiguity matrices:

$$\mathbf{\Delta}_{B^{(R)}} = \left[\text{diag}(\hat{\mathbf{B}}_{1.}^{(R)})\right]^{-1} \;,\; \mathbf{\Delta}_{B^{(T)}} = \left[\text{diag}(\hat{\mathbf{B}}_{1.}^{(T)})\right]^{-1} \tag{57}$$

and

$$\mathbf{\Delta}_W = \left[\mathbf{\Delta}_{B^{(R)}}\mathbf{\Delta}_{B^{(T)}}\right]^{-1} = \text{diag}(\hat{\mathbf{B}}_{1.}^{(R)})\,\text{diag}(\hat{\mathbf{B}}_{1.}^{(T)}). \tag{58}$$

Note that the permutation ambiguity can not be removed, which is of no practical consequence. Indeed, this ambiguity which corresponds to a permutation of the multipaths is irrelevant from an application point of view.

Finally, the rectification algorithm proposed in [31] is employed to improve the estimation of the DoA and DoD angles from the estimated Vandermonde matrices $\hat{\hat{\mathbf{B}}}^{(R)}$ and $\hat{\hat{\mathbf{B}}}^{(T)}$.

The proposed MKRF/ALS and MKRF/LS/ALS receivers are summarized in Table 3, where the noisy received signals tensor is given by:

$$\tilde{\boldsymbol{\mathcal{X}}} = \boldsymbol{\mathcal{X}} + \sigma\, \boldsymbol{\mathcal{N}}, \tag{59}$$

Remark 2. The convergence mentioned in step 9.5 of the ALS algorithm, in Table 3, is decided when the normalized difference between two estimates of the channel unfolding $\hat{\mathbf{H}}_{TsM_R \times M_T}$, at two successive iterations, is less than or equal to 10^{-6}. The maximum number of iterations for the ALS algorithm is fixed at 1000.

Remark 3. The computational complexity of the KRF algorithm is mainly due to SVD computations for calculating rank-one approximations[1], which implies the following global computational cost for the MKRF algorithm:

$$O\Big(M_T P T_S M_R \min(P, T_S M_R)\Big) + O\Big(M_T P \sum_{m=2}^{M} \min(P_m, \frac{P}{P_m})\Big). \tag{60}$$

The complexity of the MKRF/ALS receiver is given by Eq. (60) for the first stage, plus $O\Big(T_s M_R M_T L \min(T_s M_R M_T, L) + T_s M_R^2 L \min(T_s M_R^2, L) + M_R M_T L \min(M_R M_T, L)\Big)$ by iteration for the second one.

Note that the MKRF/ALS and MKRF/LS/ALS receivers have the same computational complexity, since the LS channel estimator given by Eq. (84), avoids any matrix inversion.

6. Expected CRB for the channel

The Cramer-Rao bound (CRB), defined as the inverse of the Fisher Information Matrix (FIM), provides a lower bound for the mean square error (MSE) of channel estimation in

[1]The cost of the SVD computation of an $I \times J$ matrix is given by $O\Big(IJ \min(I, J)\Big)$.

Table 3: MKRF-(LS)-ALS receivers

Inputs: Noisy received signals tensor $\tilde{\boldsymbol{\mathcal{X}}}$; coding matrix $\mathbf{C}$.

Outputs: Estimated symbol matrices $\hat{\hat{\hat{\mathbf{S}}}}^{(m)}, m \in \{2, \cdots, M\}$ and multipath parameters $(\hat{\hat{\mathbf{B}}}^{(T)}, \hat{\hat{\mathbf{B}}}^{(R)}, \hat{\hat{\mathbf{W}}})$.

First stage: MKRF algorithm

1. LS estimation of the KRP $(\mathbf{S} \diamond \mathbf{H}_{T_s M_R \times M_T})$ using (46).

2. Estimation of the matrix $\hat{\mathbf{S}}$ and of the channel unfolding $\hat{\mathbf{H}}_{T_s M_R \times M_T}$ using the KRF algorithm in Appendix A.

3. Ambiguity suppression using (53) and (54).

4. Estimation of the symbol matrices $\hat{\mathbf{S}}^{(2)}, \cdots, \hat{\mathbf{S}}^{(M)}$ using the MKRF algorithm described in Appendix B, and applied to $\hat{\hat{\mathbf{S}}}$, with ambiguity suppression for each symbol matrix using (55).

5. Projection of the estimated symbols onto the alphabet to obtain $\hat{\hat{\hat{\mathbf{S}}}}^{(m)}$.

6. Reshaping of channel estimate obtained in step 1 with the MKRF algorithm.

Second stage: LS algorithm

7. Reconstruction of the matrix $\hat{\hat{\hat{\mathbf{S}}}}$ using $\hat{\hat{\hat{\mathbf{S}}}}^{(m)}$ obtained in step 4 with the MKRF algorithm.

8. Refined channel estimation using Eq. (84).

Third stage: ALS algorithm

9.1 Initialization ($it = 0$): $\mathbf{B}_0^{(T)}$, $\mathbf{W}_0$.

9.2 Calculation of $\hat{\mathbf{B}}_{it+1}^{(R)}$ using (50).

9.3 Calculation of $\hat{\mathbf{B}}_{it+1}^{(T)}$ using (51).

9.4 Calculation of $\hat{\mathbf{W}}_{it+1}$ using (52).

9.5 Repeat steps 9.2 - 9.4 until convergence.

9.6 Ambiguity suppression using (56)-(58).

10. Application of the rectification algorithm [31] to estimate the DoA and DoD angles.

the presence of nuisance parameters corresponding to the information symbols. Let $\mathbf{h}$ be a vectorized form of the channel tensor, decomposed as $\mathbf{h} = [\bar{\mathbf{h}}^T \tilde{\mathbf{h}}^T]^T$ where $\bar{\mathbf{h}} = \mathrm{Re}(\mathbf{h})$ and $\tilde{\mathbf{h}} = \mathrm{Im}(\mathbf{h})$. The expected CRB is such that [33]:

$$\mathrm{E} \parallel \mathbf{h} - \hat{\mathbf{h}} \parallel^2 \geq \mathrm{E}_{\bar{\mathbf{h}},\tilde{\mathbf{h}},\boldsymbol{\gamma}} \Big\{ \mathrm{Trace}\{\mathrm{CRB}(\bar{\mathbf{h}})\} + \mathrm{Trace}\{\mathrm{CRB}(\tilde{\mathbf{h}})\} \Big\} \tag{61}$$

where $E[.]$ denotes the mathematical expectation, $\hat{\mathbf{h}}$ is an estimate of $\mathbf{h}$, and $\boldsymbol{\gamma}$ is the vector of nuisance parameters.

Assuming that the observations follow a circular Gaussian distribution $\mathbf{x} \sim \mathrm{CN}(\boldsymbol{\mu}, \mathbf{R})$, the FIM relatively to $\mathbf{h}$, denoted $\mathbf{F}(\mathbf{h})$, is given by the Slepian-Bangs (SB) formula [34]:

$$[\mathbf{F}(\mathbf{h})]_{k,j} = \quad 2\mathrm{Re}\Big\{ \Big(\frac{\partial \boldsymbol{\mu}}{\partial [\mathbf{h}]_k} \Big)^H \mathbf{R}^{-1} \frac{\partial \boldsymbol{\mu}}{\partial [\mathbf{h}]_j} \Big\}, \tag{62}$$

this equality being due to the fact that the noise covariance matrix $\mathbf{R}$ does not depend on the channel parameters. From the unfolding (44) of the PARAFAC model, it is easy to deduce the following other matrix unfolding of the noisy received signals:

$$\tilde{\mathbf{X}}_{KP \times T_s M_R} = (\mathbf{C} \diamond \mathbf{S}) \mathbf{H}_{M_T \times T_s M_R} + \mathbf{N}_{KP \times T_s M_R} \tag{63}$$

with $\mathbf{S} \triangleq \diamond_{m=2}^{M} \mathbf{S}^{(m)}$, and $\mathbf{N}_{KP \times T_s M_R}$ is a matrix unfolding of the additive noise tensor. Using Property (1) for vectorization, we obtain:

$$\tilde{\mathbf{x}} \triangleq \mathrm{vec}(\tilde{\mathbf{X}}_{KP \times T_s M_R}) = \Big[\mathbf{I}_{T_s M_R} \otimes (\mathbf{C} \diamond \mathbf{S}) \Big] \mathrm{vec}(\mathbf{H}_{M_T \times T_s M_R}) + \mathrm{vec}(\mathbf{N}_{KP \times T_s M_R}), \tag{64}$$

or in a more compact form:

$$\tilde{\mathbf{x}} = \mathbf{A}\mathbf{h} + \boldsymbol{\rho} \tag{65}$$

where $\mathbf{h} \triangleq \mathrm{vec}(\mathbf{H}_{M_T \times T_s M_R})$, $\boldsymbol{\rho} \triangleq \mathrm{vec}(\mathbf{N}_{KP \times T_s M_R})$ and:

$$\mathbf{A} \triangleq \mathbf{I}_{T_s M_R} \otimes \mathbf{Y} \in \mathbb{C}^{T_s M_R KP \times T_s M_R M_T} \quad , \quad \mathbf{Y} \triangleq \mathbf{C} \diamond \mathbf{S} \in \mathbb{C}^{KP \times M_T} \tag{66}$$

The symbol matrices being discrete-valued, they violate the regularity conditions of the CRB. So, they are viewed as random nuisance parameters, and we define $\boldsymbol{\gamma} \triangleq \mathrm{vec}(\mathbf{S})$. For a given realization of the symbol matrices, we have $\tilde{\mathbf{x}} \sim \mathrm{CN}(\mathbf{A}\mathbf{h}, \sigma^2 \mathbf{I})$, where σ^2 is the variance of each element of the noise tensor. Using the SB formula, we get:

$$\frac{\partial \boldsymbol{\mu}}{\partial \bar{\mathbf{h}}} = \mathbf{A} \ ; \ \frac{\partial \boldsymbol{\mu}}{\partial \tilde{\mathbf{h}}} = i\mathbf{A}. \tag{67}$$

Then, the inverse of the FIM is given by:

$$[\mathbf{F}(\mathbf{h})]^{-1} = \frac{\sigma^2}{2}\begin{bmatrix} \mathrm{Re}(\mathbf{A}^H\mathbf{A}) & -\mathrm{Im}(\mathbf{A}^H\mathbf{A}) \\ \mathrm{Im}(\mathbf{A}^H\mathbf{A}) & \mathrm{Re}(\mathbf{A}^H\mathbf{A}) \end{bmatrix}^{-1}. \tag{68}$$

Application of the Banachiewicz-Schur formula (4) gives:

$$\mathrm{CRB}(\bar{\mathbf{h}}) = \frac{\sigma^2}{2}\Big([\mathrm{Re}(\mathbf{A}^H\mathbf{A})]^{-1} - \frac{2}{\sigma^2}[\mathrm{Re}(\mathbf{A}^H\mathbf{A})]^{-1}\mathrm{Im}(\mathbf{A}^H\mathbf{A})\,\mathrm{CRB}(\bar{\mathbf{h}})\,\mathrm{Im}(\mathbf{A}^H\mathbf{A})[\mathrm{Re}(\mathbf{A}^H\mathbf{A})]^{-1}\Big) \tag{69}$$

and

$$\mathrm{CRB}(\tilde{\mathbf{h}}) = \frac{\sigma^2}{2}\Big(\mathrm{Re}(\mathbf{A}^H\mathbf{A}) + \mathrm{Im}(\mathbf{A}^H\mathbf{A})[\mathrm{Re}(\mathbf{A}^H\mathbf{A})]^{-1}\mathrm{Im}(\mathbf{A}^H\mathbf{A})\Big)^{-1}. \tag{70}$$

Using definition (66) and Property (2) of the Kronecker product leads to:

$$\mathbf{A}^H\mathbf{A} = \mathbf{I}_{T_sM_R} \otimes \mathbf{Y}^H\mathbf{Y}. \tag{71}$$

From this expression, we deduce that the product $\mathbf{A}^H\mathbf{A}$ is a block-diagonal matrix of dimension $T_sM_RM_T \times T_sM_RM_T$, with $\mathbf{Y}^H\mathbf{Y}$ as diagonal blocks, and we have the following relations:

$$\mathrm{Re}(\mathbf{A}^H\mathbf{A}) = \mathbf{I}_{T_sM_R} \otimes \mathrm{Re}(\mathbf{Y}^H\mathbf{Y}) \ , \ \ \mathrm{Im}(\mathbf{A}^H\mathbf{A}) = \mathbf{I}_{T_sM_R} \otimes \mathrm{Im}(\mathbf{Y}^H\mathbf{Y}). \tag{72}$$

Using Property (3) of the Khatri-Rao product gives:

$$\mathbf{Y}^H\mathbf{Y} = (\mathbf{C} \diamond \mathbf{S})^H(\mathbf{C} \diamond \mathbf{S}) = \mathbf{C}^H\mathbf{C} \odot \mathbf{S}^H\mathbf{S}. \tag{73}$$

The coding matrix $\mathbf{C}$ being assumed to be column-orthonormal, as defined in (45), we have $\mathbf{C}^H\mathbf{C} = \mathbf{I}_{M_T}$, and Eq. (73) becomes:

$$\mathbf{Y}^H\mathbf{Y} = \mathbf{I}_{M_T} \odot \mathbf{S}^H\mathbf{S} = \mathrm{diag}\Big[(\mathbf{S}^H\mathbf{S})_{1,1}, \cdots, (\mathbf{S}^H\mathbf{S})_{M_T,M_T}\Big], \tag{74}$$

that is, $\mathbf{Y}^H\mathbf{Y} \in \mathbb{C}^{M_T \times M_T}$ is a diagonal matrix whose diagonal elements are given by:

$$(\mathbf{S}^H\mathbf{S})_{m_T,m_T} = \prod_{m=2}^{M} (\mathbf{S}^{(m)H}\mathbf{S}^{(m)})_{m_T,m_T} \text{ with } m_T \in \langle M_T \rangle. \tag{75}$$

Defining the symbol matrix $\mathbf{S}^{(m)}$ as:

$$\mathbf{S}^{(m)} = \begin{pmatrix} 1 & \cdots & 1 \\ \vdots & \ddots & \vdots \\ s^{(m)}_{P_m,1} & \cdots & s^{(m)}_{P_m,M_T} \end{pmatrix}, \tag{76}$$

it is easy to deduce that:

$$(\mathbf{S}^{(m)H}\mathbf{S}^{(m)})_{m_T,m_T} = 1 + |s^{(m)}_{2,m_T}|^2 + \cdots + |s^{(m)}_{P_m,m_T}|^2. \tag{77}$$

Considering that the symbols are uniformly randomly drawn from 16QAM modulation with unit energy, we have $|s^{(m)}_{p_m,m_T}|^2 = 1$ for $m \in \{2,\cdots,M\}, m_T \in \langle M_T\rangle$ and $p_m \in \langle P_m\rangle$. Taking Eqs. (77) and (75) into account leads to:

$$(\mathbf{S}^{(m)H}\mathbf{S}^{(m)})_{m_T,m_T} = P_m \ , \ \forall \ m_T \in \langle M_T\rangle \tag{78}$$

$$(\mathbf{S}^{H}\mathbf{S})_{m_T,m_T} = P, \tag{79}$$

which means that $(\mathbf{S}^H\mathbf{S})_{m_T,m_T}$ is independent of m_T, and Eqs. (74) and (71) give:

$$\mathbf{Y}^H\mathbf{Y} = P\ \mathbf{I}_{M_T} \tag{80}$$

$$\mathbf{A}^H\mathbf{A} = P\ \mathbf{I}_{T_sM_RM_T}, \tag{81}$$

implying that $\mathrm{Re}(\mathbf{A}^H\mathbf{A}) = \mathbf{A}^H\mathbf{A}$ and $\mathrm{Im}(\mathbf{A}^H\mathbf{A}) = \mathbf{0}$. Expressions (69) and (70) simplify as:

$$\mathrm{CRB}(\bar{\mathbf{h}}) = \frac{\sigma^2}{2}[\mathrm{Re}(\mathbf{A}^H\mathbf{A})]^{-1} = \frac{\sigma^2}{2P}\mathbf{I}_{T_sM_RM_T} = \mathrm{CRB}(\tilde{\mathbf{h}}) \tag{82}$$

and the CRB is given by:

$$\mathrm{CRB} = \mathrm{Trace}\{\mathrm{CRB}(\bar{\mathbf{h}})\} + \mathrm{Trace}\{\mathrm{CRB}(\tilde{\mathbf{h}})\} = \frac{\sigma^2}{P}T_sM_RM_T. \tag{83}$$

It is worth noting that $\mathbf{Y}^H\mathbf{Y}$ and subsequently $\mathbf{A}^H\mathbf{A}$, given in (80) and (81) respectively, are independent of the channel parameters $\mathbf{h}$ to be estimated due to the linearity of the model (65) with respect to $\mathbf{h}$. Moreover, these quantities are also independent of the information symbols because $\mathbf{S}^H\mathbf{S}$ only depends on the dimensions of $\mathbf{S}$. That explains why the expected CRB defined in (61) is invariant with respect to the model and nuisance parameters.

It is also important to note that the parameters in the numerator of the CRB are all related to the channel design parameters (M_R, M_T) and the number T_s of repetitions. An increase of these parameters degrades the estimation accuracy. However, to mitigate this increase of the CRB, it is possible to increase M, the number of symbol matrices, or/and to increase P_m, the number of data streams in the m-th symbol matrix, for $m \in \{2,\cdots,M\}$.

From its expression (83), we can conclude that the CRB depends on the dimensions P_m (for $m \in \{2, \cdots, M\}$) and M of $\mathbf{S}$, the noise variance σ^2 and the channel dimensions (T_s, M_R, M_T). So, for a given system configuration, the CRB is invariant with respect to the model and nuisance parameters, which implies there is no need to use Monte Carlo runs for computing the mathematical expectation (61), as illustrated by means of the simulations.

Finally, as expected, the CRB is proportional to σ^2 and (T_s, M_R, M_T), while it is inversely proportional to $(P_m, m \in \{2, \cdots, M\}; M)$, which can be explained by the use of the MKRF estimator. Indeed, channel estimation performance is improved when P_m, and M are increased because an increase of the dimensions of $\mathbf{S}$ implies a redundancy augmentation of the channel parameters through the MKRP in Eq. (44).

Remark 4. From Eq. (65), one can derive the following expression of the LS estimator of the channel in a vectorized form: $\hat{\mathbf{h}} = \mathbf{A}^{\dagger}\tilde{\mathbf{x}}$ with $\mathbf{A}^{\dagger} = (\mathbf{A}^H\mathbf{A})^{-1}\mathbf{A}^H$. Taking Eqs. (66) and (81) into account allows us to simplify this estimator as:

$$\hat{\mathbf{h}} = P\Big(\mathbf{I}_{T_s M_R} \otimes \hat{\hat{\mathbf{Y}}}^H\Big)\tilde{\mathbf{x}}, \tag{84}$$

where $\hat{\hat{\mathbf{Y}}} = \mathbf{C} \diamond \hat{\hat{\mathbf{S}}}$ and $\hat{\hat{\mathbf{S}}}$ is the matrix $\mathbf{S}$ reconstructed using the estimated symbol matrices $\hat{\hat{\mathbf{S}}}^{(m)}$ after projection.

7. Simulation results

In this section, we evaluate the performance of the proposed semi-blind receivers based on KRST/MKRSM coding. Monte Carlo simulation results are provided to illustrate: i) the impact of the design parameters M, M_T, K, T_s and M_R, on the symbol error rate (SER) performance; ii) the comparison of the SER performance obtained with the MKRF algorithm and the zero forcing (ZF) receiver corresponding to a perfect a priori knowledge of the channel; iii) the performance of the semi-blind MKRF/ALS receiver and of its improved version MKRF/LS/ALS, for the estimation of the multipath parameters.

We consider ULAs with M_T and M_R elements at the transmitter and the receiver, respectively. In general, the multipath system is simulated with $L = 2$, $(\varphi_1, \theta_1) = (70°, 20°)$ and $(\varphi_2, \theta_2) = (30°, 60°)$. Symbols of the matrices $\mathbf{S}^{(m)} \in \mathbb{C}^{P_m \times M_T}$, with $m \in [2, M]$, are

randomly drawn from the 16QAM alphabet, with a uniform distribution. The coding matrix $\mathbf{C} \in \mathbb{C}^{K \times M_T}$, assumed to be known at the receiver, is chosen as a truncated Fourier matrix. The fading coefficient matrix $\mathbf{W} \in \mathbb{C}^{T_s \times M_T}$ is randomly drawn from a complex Gaussian distribution $CN(0,1)$. The SER and mean square error (MSE) curves are plotted versus the signal to noise ratio (SNR). The entries of the additive noise tensor are randomly drawn with a complex Gaussian distribution $CN(0,1)$.

For a specified value τ of the SNR in dB, the factor σ is determined such as:

$$\sigma = \frac{1}{10^{\tau/20}} \frac{\| \boldsymbol{\mathcal{X}} \|_F}{\| \boldsymbol{\mathcal{N}} \|_F}. \tag{85}$$

Simulation results are obtained by averaging the results of $M_c = 10^3$ Monte Carlo runs. Each Monte Carlo run corresponds to different realizations of the symbol matrices, the channel fading coefficients, and the additive noise. The channel MSE obtained with MKRF is calculated as:

$$\text{MSE}_{\mathbf{H}} = \frac{1}{M_c} \sum_{mc=1}^{M_c} \| (\mathbf{H}_{mc})_{T_s M_R \times M_T} - (\hat{\mathbf{H}}_{mc})_{T_s M_R \times M_T} \|_F^2 . \tag{86}$$

7.1. Impact of the design parameters

We first evaluate the impact of the number M of symbol matrices. Fig. 3 compares the SER performance obtained with the MKRF algorithm for $M \in \{2, 4, 5\}$ using 4QAM and 16QAM. From this figure, we can conclude that increasing the value of M improves the SER performance thanks to the MKRSM coding. Indeed, an increase of the number of symbol matrices induces a redundancy augmentation via the MKRSM coding in Eq. (46). As expected, the SER performance is better when using 4QAM, the decoding being easier with 4QAM than with 16QAM.

For the same reason of redundancy augmentation, the channel MSE plotted on Fig. 4 is also improved when M is increased. Indeed, the channel unfolding $\mathbf{H}_{T_s M_R \times M_T}$ is jointly estimated with the MKRP matrix $\mathbf{S} \triangleq \diamond_{m=2}^{M} \mathbf{S}^{(m)}$ by means of the MKRF algorithm. Increasing M implies an increase of P, with $P_m = 3$ for $m \in \{2, \cdots, M\}$, and therefore more diversity to estimate the channel unfolding. Thus, increasing M improves the estimation of $\mathbf{H}_{T_s M_R \times M_T}$. The expected CRB is also plotted for reference. We verify that the CRB decreases when M and therefore P increases, according to Eq. (83). Use of the refined

$$L = 2; M_R = M_T = K = 3; T_s = 5; P_m = 3$$

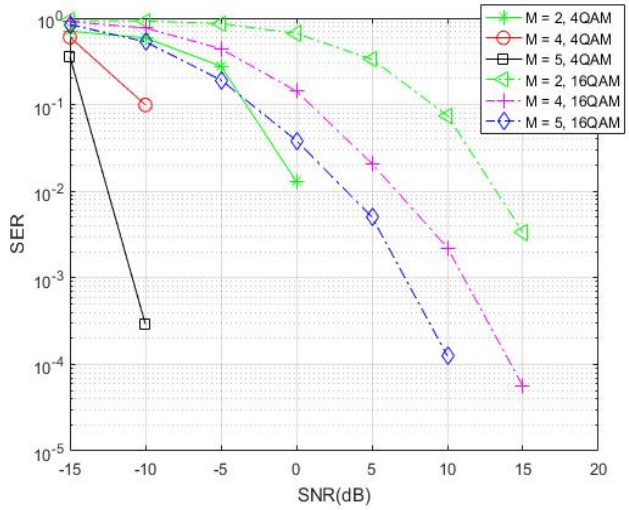

Figure 3: Impact of M on SER with MKRF

channel estimation allows to improve the efficiency of the rectified MKRF/LS/ALS receiver as clearly shown on Fig. 4, the $MSE_{\mathbf{H}}$ being very close to the CRB on a large SNR range.

$$L = 2; M_R = M_T = K = 3; T_s = 5; P_m = 3$$

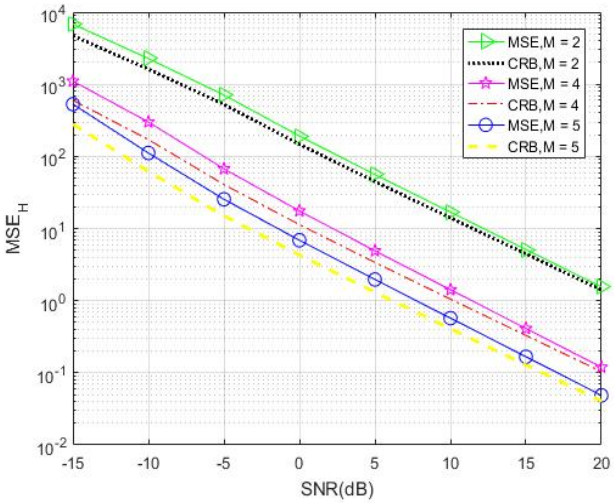

Figure 4: Impact of M on channel MSE with rectified MKRF/LS/ALS receiver

We now fix $M = 4$ for the rest of this subsection. With the next experiment, we evaluate the impact of the number M_T of transmit antennas. For $M_T \in \{2, 5, 10\}$, Fig. 5 shows that an increase of M_T does not significantly modify the SER performance due to the fact that the MKRF algorithm operates separately for each column $m_T \in \langle M_T \rangle$ in (46), the processing

of each column being independent of the others. Indeed, considering the KRF described in Appendix A, we can note that the rank-one approximations are computed column by column, which explains why the estimation results do not depend on the number of columns.

$$L = 2; M_R = 3; K = 10; T_s = 5; M = 4; P_m = 3$$

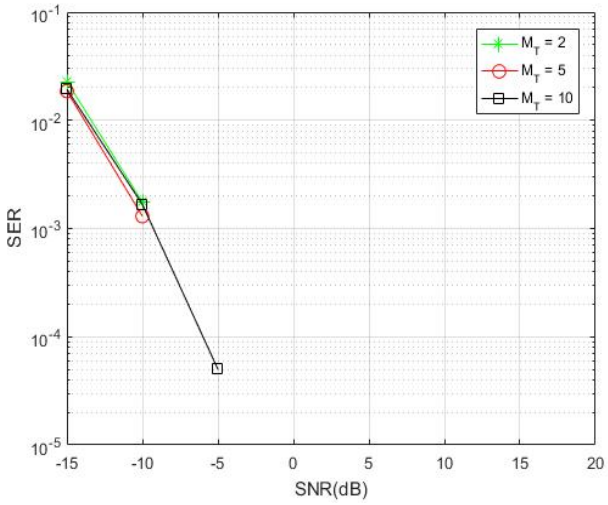

Figure 5: Impact of M_T on SER with the MKRF algorithm

Fig. 6 shows the coding length $K \in \{5, 10, 15\}$ also does not significantly modify the SER performance. Indeed, this dimension is an internal parameter in the matrix product on the right member of (46), and consequently does not modify the number of equations used for parameter estimation, which explains the low dependency of the SER with respect to K.

Finally, the space-time diversity introduced by means of the product $T_s M_R$ corresponding to channel dimensions is analyzed. For $(T_s; M_R) \in \{(2; 4), (3; 8), (5; 10)\}$, Fig. 7 shows that greater is this product, smaller is the SER due to more redundancy in the transmitted symbols, caused by the time (T_s) and space (M_R) diversities in the Khatri-Rao product (46). Indeed, an increase of the product $T_s M_R$ implies more redundancy to estimate the transmitted symbols, and consequently an improvement of the SER performance.

7.2. Comparison of the MKRF algorithm with the ZF receiver

We fix $M = 4$, $P_2 = 3, P_3 = 5, P_4 = 8$, with the following aims: i) to compare the global SERs obtained with the ZF receiver (i.e., when assuming a perfect a priori knowledge of the channel at the receiver) and the MKRF algorithm, ii) to evaluate the influence of the symbol

$$L = 2; M_R = M_T = 3; T_s = 5; M = 4; P_m = 3$$

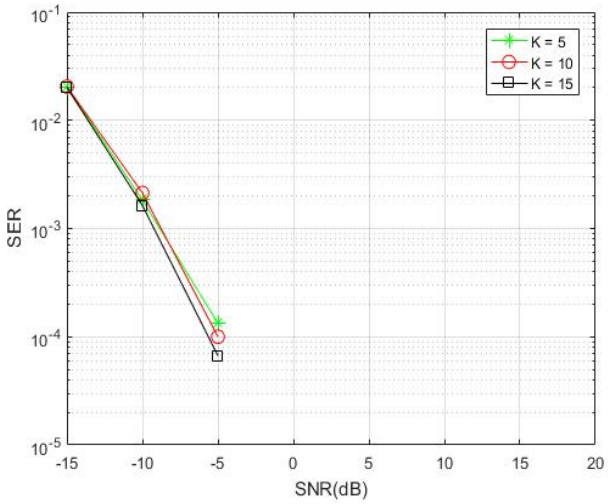

Figure 6: Impact of K on SER obtained with the MKRF algorithm

$$L = 2; M_T = K = 3; M = 4; P_m = 3$$

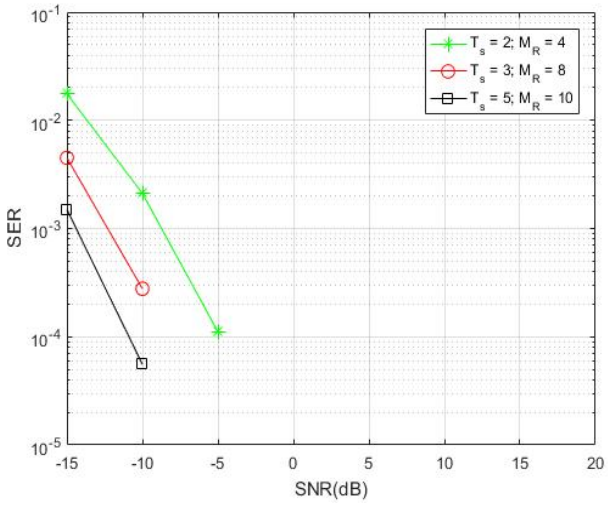

Figure 7: Impact of $T_s M_R$ on SER obtained with the MKRF algorithm

matrices dimensions P_m. Using the following matrix unfolding of the received signals tensor:

$$\mathbf{X}_{P \times T_s M_R K} = \mathbf{S}\Big(\mathbf{H}_{T_s M_R \times M_T} \diamond \mathbf{C}\Big)^T, \tag{87}$$

one can deduce the equation of the ZF receiver to estimate the matrix $\mathbf{S}$ and then the symbol matrices $\mathbf{S}^{(m)}, m \in \{2, \cdots, M\}$:

$$\hat{\mathbf{S}} = \tilde{\mathbf{X}}_{P \times T_s M_R K} \Big[\Big(\mathbf{H}_{T_s M_R \times M_T} \diamond \mathbf{C}\Big)^T\Big]^{\dagger}. \tag{88}$$

Fig. 8 shows that the SER obtained with the MKRF algorithm is very close to the one

$$L = 2; M_R = M_T = K = 3; = T_s = 5; M = 4; P_2 = 3; P_3 = 5; P_4 = 8$$

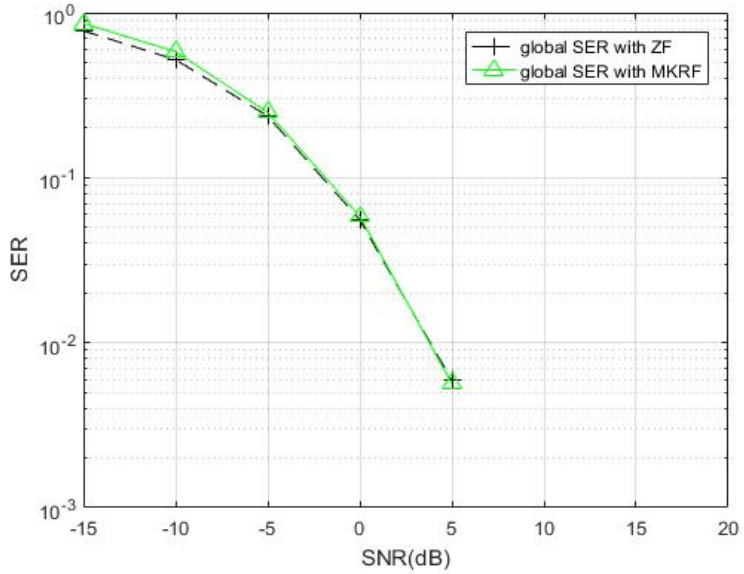

Figure 8: Comparison of global SERs using the ZF and MKRF algorithms

$$L = 2; M_R = M_T = K = 3; = T_s = 5; M = 4; P_2 = 3; P_3 = 5; P_4 = 8$$

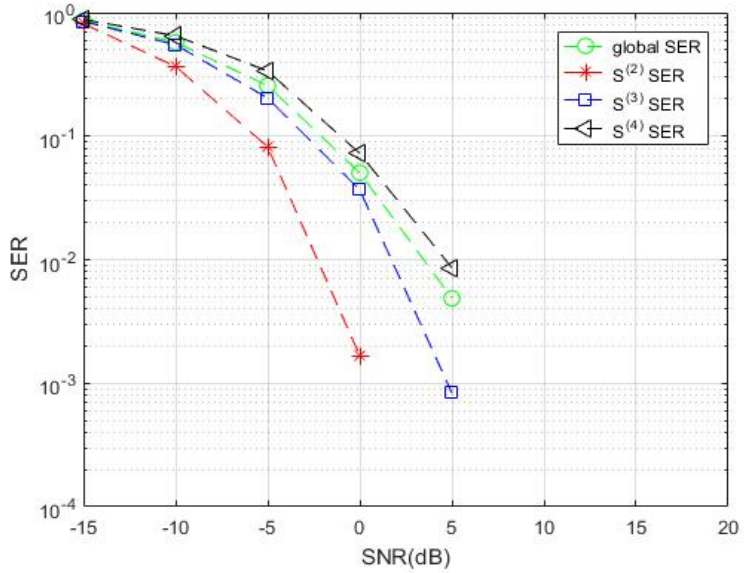

Figure 9: Comparison of individual SERs using the MKRF algorithm

obtained with the ZF receiver, which corroborates the excellent performance of the MKRF algorithm. In Fig. 9, we compare the individual SERs of each symbol matrix estimated using

the MKRF algorithm. As expected, from these simulation results, we can conclude that the best individual SER is obtained for the symbol matrix $\mathbf{S}^{(m)}$ with the smallest dimension P_m due to a greater redundancy provided by the other symbol matrices, this redundancy being proportional to the product $\prod_{\substack{n=2 \\ n \neq m}}^{M} P_n$. The global SER is close to the individual SER of the symbol matrix with the greatest dimension P_m.

7.3. Channel and multipath parameters estimation

In this section, we evaluate the performance of the proposed semi-blind receivers in terms of root mean square error (RMSE) of the estimated angles, the channel MSE ($MSE_{\mathbf{H}}$), and the received signals MSE ($MSE_{\mathbf{X}}$) reconstructed using the estimated channel and information symbols. The design parameters are fixed with the following values: $M = 4, P_2 = 3, P_3 = 5, P_4 = 8$.

The total RMSE of the estimated angles, using the MKRF/ALS and MKRF/LS/ALS receivers, with and without rectification, is calculated as:

$$\text{RMSE} = \frac{1}{M_c} \sum_{mc=1}^{M_c} \sqrt{\frac{1}{L} \sum_{l=1}^{L} (\varphi_l - \hat{\varphi}_{l_{mc}})^2 + (\theta_l - \hat{\theta}_{l_{mc}})^2}. \tag{89}$$

With the MKRF/ALS receiver, the angle of each column of the estimated steering matrices is extracted from the second row of these matrices, while with the MKRF/LS/ALS, these angles are estimated using the RecALS method described in [31].

From Fig. 10, one can conclude that the RMSE decreases when the SNR increases, and that the MKRF/LS/ALS receiver gives much better performance than the MKRF/ALS one, corroborating the important role played by the refinement of channel estimation using Eq. (84). Moreover, the rectification algorithm allows to significantly improve the angle estimation with both receivers.

We now evaluate the impact of the number L of paths on RMSE, for $L \in \{2, 4, 6\}$. As expected, on Fig. 11, one observes that the best RMSE is obtained for the smallest value of L, since the channel estimation problem is more challenging when the number of paths increases, implying more channel coefficients to be estimated, and therefore less accuracy on angle estimation. However, when L is increased from 2 to 6, it can be observed that

the SNR gap is around $2dB$, illustrating the system robustness with respect to the number of paths. One can also conclude that the rectification algorithm clearly improves the angle estimation accuracy with a SNR gap of around $5dB$ for a fixed angle RMSE, with and without rectification.

$$L = 2; M_R = M_T = K = 3; T_s = 5; M = 4; P_2 = 3; P_3 = 5; P_4 = 8$$

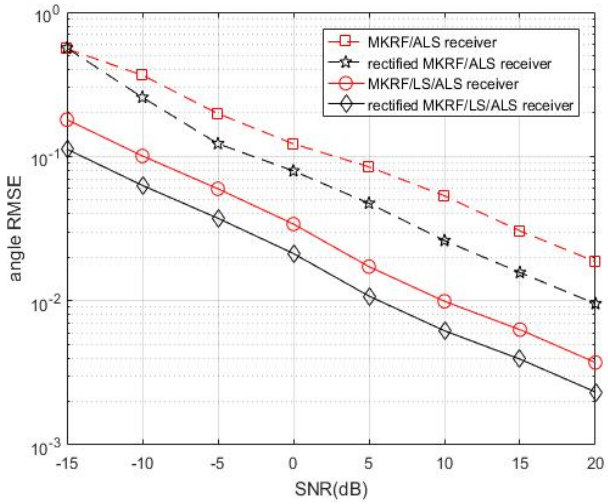

Figure 10: Angle RMSE with MKRF/ALS and MKRF/LS/ALS receivers

$$M_R = M_T = K = 3; T_s = 5; M = 4; P_2 = 3; P_3 = 5; P_4 = 8$$

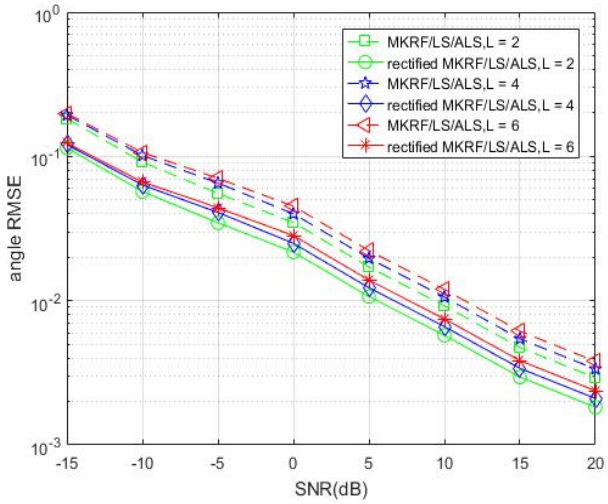

Figure 11: Impact of L on angle RMSE with MKRF/LS/ALS receiver

We now compare channel $MSE_{\mathbf{H}}$ obtained with different receivers: i) the MKRF algorithm; ii) the MKRF/ALS receiver without and with rectification; iii) the supervised LS

receiver which corresponds to the LS algorithm applied to Eq. (65), with the exact symbols, i.e., using a training sequence; iv) the MKRF/LS receiver which corresponds to the refined channel estimation using Eq. (84); v) the complete MKRF/LS/ALS receiver, without and with rectification.

$$L = 2; M_R = M_T = K = 3; T_s = 5; M = 4; P_2 = 3; P_3 = 5; P_4 = 8$$

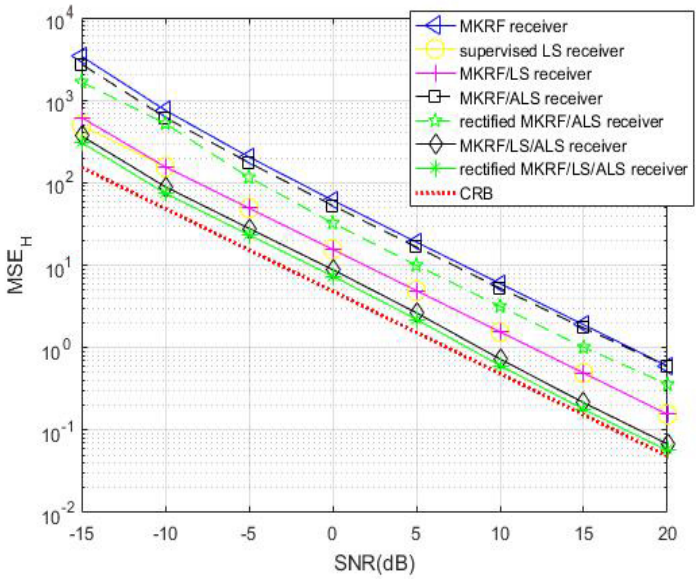

Figure 12: Comparison of $MSE_{\mathbf{H}}$ with the CRB for different receivers (with and without rectification)

Analyzing the results plotted on Fig. 12, one can conclude that, for $\tau \geq -5$dB, the MKRF/LS receiver gives the same channel $\text{MSE}_{\mathbf{H}}$ as the one obtained with the supervised LS receiver (i.e., Eq. (84) with perfect a priori knowledge of $\mathbf{S}$ instead of the reconstructed $\hat{\hat{\mathbf{S}}}$). That corroborates the very good estimation of the symbol matrices with the MKRF algorithm. Fig. 12 also shows that the best $\text{MSE}_{\mathbf{H}}$ performance is obtained with the MKRF/LS/ALS receiver, illustrating the performance gain brought by the refined channel estimator, in comparison with the channel estimate provided by the MKRF algorithm, for estimating the multipath parameters with the ALS algorithm and then reconstructing the final channel estimate. Finally the rectification algorithm, combined with the MKRF/ALS receiver allows to significantly improve the $\text{MSE}_{\mathbf{H}}$, while this improvement is much less marked with the MKRF/LS/ALS receiver, the $\text{MSE}_{\mathbf{H}}$ being already very close to the expected CRB, on a large SNR range, for this last receiver.

On the other hand, applying the ALS algorithm to a badly estimated channel by means of the MKRF algorithm does not significantly improve the system performance. The rectification algorithm does not bring a great improvement to the MKRF/ALS receiver.

Finally, in Fig. 13, we compare the $MSE_{\mathbf{X}}$ of the reconstructed received signals, obtained with the MKRF, MKRF/LS, MKRF/ALS and MKRF/LS/ALS receivers, without and with rectification. This $MSE_{\mathbf{X}}$ is calculated by means of the following expression:

$$\mathrm{MSE}_{\mathbf{X}} = \frac{1}{M_c} \sum_{mc=1}^{M_c} \| \, (\tilde{\mathbf{X}}_{mc})_{T_s \, M_R \times KP} - (\hat{\tilde{\mathbf{H}}}_{mc})_{T_s M_R \times M_T} \Big(\mathbf{C} \diamond \hat{\tilde{\mathbf{S}}}_{mc}^{(2)} \diamond \cdots \diamond \hat{\tilde{\mathbf{S}}}_{mc}^{(M)} \Big)^T \, \|_F^2 \qquad (90)$$

From this figure, one can conclude that the MKRF/LS receiver outperforms the MKRF receiver and that the rectified MKRF/LS/ALS receiver gives the best $MSE_{\mathbf{X}}$ performance owing to the refined LS channel estimation. These results corroborate the previous conclusions concerning the channel $MSE_{\mathbf{H}}$ in Fig. 12 and the angle $RMSE$ in Fig. 10. We also note that the ALS algorithm combined with the MKRF one does not provide a significant improvement of the reconstructed tensor of received signals $MSE_{\mathbf{H}}$, the channel being not well estimated by means of the MKRF algorithm. Note that all the receivers using the rectification algorithm improve angle estimation.

8. Conclusion

A MIMO communication system combining KRST and MKRSM codings has been proposed in a time varying multipath context. Considering the Khatri-Rao products of $M-1$ symbol matrices, we have shown that the received signals form a $(M+2)$-order tensor which satisfies a generalized nested PARAFAC model. This extension of the nested PARAFAC model has been considered in more detail for a $(M+N)$-order tensor, and various parameter estimation algorithms have been discussed.

Semi-blind receivers allowing to jointly estimate the information symbols and the multipath parameters have been developed combining the MKRF algorithm for symbols and channel estimation, with the ALS algorithm for multipath parameters estimation, which gives the MKRF/ALS receiver. A refined solution has also been proposed using a very simple LS channel estimator which takes the column-orthonormal assumption on the coding

$$L = 2; M_R = M_T = K = 3; T_s = 5; M = 4; P_2 = 3; P_3 = 5; P_4 = 8$$

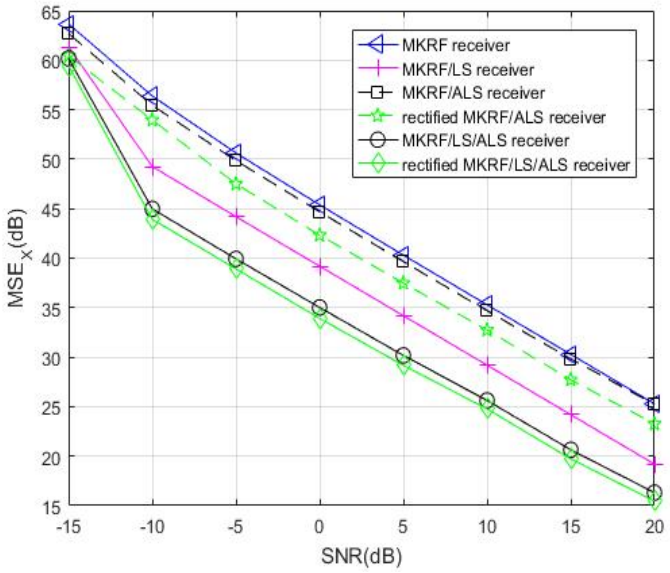

Figure 13: Comparison of $MSE_{\mathbf{X}}$ obtained with different receivers (with and without rectification)

matrix and the QAM modulation into account. That leads to the MKRF/LS/ALS receiver. Both receivers include a suppression of scalar ambiguities and a rectification algorithm to improve the accuracy of the DoD and DoA angles estimation by taking the Vandermonde structure of the steering matrices into account. The computational complexity of the receivers has been analyzed. The expected CRB that provides a lower bound for channel MSE has been established. The derived expected CRB follows a compact closed-form expression. As expected, it is proportional to the noise variance and the channel dimensions, whereas it is inversely proportional to the dimensions of the symbol matrices.

Monte Carlo simulation results have corroborated that an increase of the number of symbol matrices in the MKRSM coding improves the SER and the channel MSE performances. Moreover, the simulations have allowed to conclude that the length K of the time spreading of the KRST coding and the number M_T of transmit antennas do not significantly impact the SER performance. The simulation results have illustrated the very good SER performance obtained with the closed-form MKRF algorithm. It was also shown that the channel MSE obtained using the refined LS channel estimator which exploits the symbols estimated by means of the MKRF algorithm is very close to the channel MSE obtained with the super-

vised (pilots-based) receiver, the corresponding channel MSE being very close to the CRB. Finally, the simulation results have corroborated that the rectification algorithm contributes to a significant performance improvement for angle estimation.

References

9. Bibliography

[1] R. A. Harshman, Foundations of the PARAFAC procedure: Models and conditions for an" explanatory" multimodal factor analysis, UCLA Working Papers in Phonetics 16 (1970) 1–84.

[2] G. Favier, A. L. F. de Almeida, Overview of constrained PARAFAC models, EURASIP J. Advances in Signal Processing (2014).

[3] A. L. F. de Almeida, G. Favier, Double Khatri-Rao space-time-frequency coding using semi-blind PARAFAC based receiver, IEEE Signal Processing Letters 20 (2013) 471–474.

[4] L. R. Ximenes, G. Favier, A. L. F. de Almeida, Semi-blind receivers for non-regenerative cooperative MIMO communications based on nested PARAFAC modeling, IEEE Tr. on Signal Processing 63 (2015) 4985–4998.

[5] L. R. Ximenes, G. Favier, A. L. F. de Almeida, Closed-form semi-blind receiver for MIMO relay systems using double Khatri–Rao space-time coding, IEEE Signal Processing Letters 23 (2016) 316–320.

[6] W. Freitas, G. Favier, A. L. F. de Almeida, Sequential closed-form semi-blind receiver for space-time coded multihop relaying systems, IEEE Signal Processing Letters 24 (2017) 1773–1777.

[7] M. N. da Costa, G. Favier, J.-M. Romano, Tensor modelling of MIMO communication systems with performance analysis and Kronecker receivers, Signal Processing 145 (2018) 304–316.

[8] A. L. F. de Almeida, G. Favier, J. P. C. L. da Costa, J. C. M. Mota, Overview of tensor decompositions with applications to communications, Chapter 12 in Signals and Images: Advances and Results in Speech, Estimation, Compression, Recognition, Filtering, and Processing, CRC-Press, 2016.

[9] G. Favier, C. A. R. Fernandes, A. L. F. de Almeida, Nested Tucker tensor decomposition with application to MIMO relay systems using tensor space-time coding (TSTC), Signal Processing 128 (2016) 318–331.

[10] D. Sousa Rocha, C. A. R. Fernandes, G. Favier, MIMO multi-relay systems with tensor space-time coding based on coupled nested Tucker decomposition, Digital Signal Processing 89 (2019) 170–185.

[11] Y. Zniyed, R. Boyer, A. L. F. de Almeida, G. Favier, Tensor-train modeling for MIMO-OFDM tensor coding-and-forwarding relay systems, in: 2019 EUSIPCO.

[12] G. Favier, M. N. Da Costa, A. L. F. de Almeida, J. M. T. Romano, Tensor space–time (TST) coding for MIMO wireless communication systems, Signal Processing 92 (2012) 1079–1092.

[13] G. Favier, A. L. F. de Almeida, Tensor space-time-frequency coding with semi-blind receivers for MIMO wireless communication systems, IEEE Tr. on Signal Processing 62 (2014) 5987–6002.

[14] W. Freitas, G. Favier, A. L. F. de Almeida, Generalized Khatri-Rao and Kronecker space-time coding for MIMO relay systems with closed-form semi-blind receivers, Signal Processing 151 (2018) 19–31.

[15] H. Krim, M. Viberg, Two decades of array signal processing research: the parametric approach, IEEE Signal Processing Magazine 13 (1996) 67–94.

[16] J. Li, P. Stoica, MIMO radar with colocated antennas, IEEE Signal Processing Magazine 24 (1996) 106–114.

[17] R. Schmidt, Multiple emitter location and signal parameter estimation, IEEE Tr. on Antennas and Propagation 34 (1986) 276–280.

[18] R. Roy, T. Kailath, ESPRIT-estimation of signal parameters via rotational invariance techniques, IEEE Tr. on Acoustics, Speech, and Signal Processing 37 (1989) 984–995.

[19] D. Nion, N. Sidiropoulos, Tensor algebra and multidimensional harmonic retrieval in signal processing for MIMO radar, IEEE Tr. on Signal Processing 58 (2010) 5693–5705.

[20] R. Boyer, Performance bounds and angular resolution limit for the moving colocated MIMO radar, IEEE Tr. on Signal Processing 59 (2011) 1539–1552.

[21] X. Wang, W. Wang, J. Liu, Q. Liu, B. Wang, Tensor-based real-valued subspace approach for angle estimation in bistatic MIMO radar with unknown mutual coupling, Signal Processing 116 (2015) 152–158.

[22] B. Xu, Y. Zhao, Z. Cheng, H. Li, A novel unitary PARAFAC method for DOD and DOA estimation in bistatic MIMO radar, Signal Processing 138 (2017) 273–279.

[23] F. Wen, X. Xiong, Z. Zhang, Angle and mutual coupling estimation in bistatic MIMO radar based on PARAFAC decomposition, Digital Signal Processing 65 (2017) 1–10.

[24] Y. Guo, X. Wang, W. Wang, M. Huang, C. Shen, C. Cao, G. Bi, Tensor-based angle estimation approach for strictly noncircular sources with unknown mutual coupling in bistatic MIMO radar, Sensors 18 (2018) 1–14.

[25] B. Yao, Z. Dong, W. Liu, Effective joint DOA-DOD estimation for the coexistence of uncorrelated and coherent signals in massive multi-input multi-output array systems, EURASIP Journal on Advances in Signal Processing (2018) 64.

[26] P. R. B. Gomes, A. L. F. de Almeida, J. P. C. L. da Costa, R. T. de Sousa, A nested-PARAFAC based approach for target localization in bistatic MIMO radar systems, Digital Signal Processing 89 (2019) 40–48.

[27] A. L. F. de Almeida, G. Favier, J. C. M. Mota, Multipath parameter estimation of time-varying space-time communication channels using parallel factor analysis, in: (2006) IEEE Int. Conf. on Acoustics Speech and Signal Processing, volume 4.

[28] C. E. R. Fernandes, G. Favier, J. C. M. Mota, Blind multipath MIMO channel parameter estimation using the PARAFAC decomposition, in: 2009 IEEE Int. Conf. on Communications.

[29] Y. Zniyed, R. Boyer, A. L. F. de Almeida, G. Favier, Tensor train representation of MIMO channels using the JIRAFE method, Signal Processing 171 (2020).

[30] N. D. Sidiropoulos, R. S. Budampati, Khatri-Rao space-time codes, IEEE Tr. on Signal Processing 50 (2002) 2396–2407.

[31] R. Boyer, P. Comon, Rectified ALS algorithm for multidimensional harmonic retrieval, in: Sensor Array and Multichannel Signal Proc. Workshop (SAM), IEEE, pp. 1–5.

[32] J. B. Kruskal, Three-way arrays: rank and uniqueness of trilinear decompositions, with application to arithmetic complexity and statistics, Linear Algebra and its Applications 18 (1977) 95–138.

[33] Y. C. Eldar, Rethinking biased estimation: Improving maximum likelihood and the Cramer Rao bound, Foundations and Trends in Signal Processing (2008) 305–449.

[34] P. Stoica, R. L. Moses, Spectral analysis of signals, Wiley, 2005.

[35] A. Y. Kibangou, G. Favier, Non-iterative solution for PARAFAC with a Toeplitz matrix factor, in: (2009) 17th European Signal Processing Conference, pp. 691–695.

[36] G. Favier, Matrices and tensors in signal processing, volume 2, Wiley, to appear in 2020.

Appendix A. Khatri-Rao factorization (KRF) algorithm

Let $\mathbf{A} \in \mathbb{C}^{I\times L}$, $\mathbf{B} \in \mathbb{C}^{J\times L}$, and $\mathbf{Y} = \mathbf{A} \diamond \mathbf{B} \in \mathbb{C}^{IJ\times L}$. The KRF algorithm allows to estimate the matrix factors $\mathbf{A}$ and $\mathbf{B}$ from their Khatri-Rao product (KRP) $\mathbf{Y}$ by operating

column by column [35]. The method consists in building a rank-one matrix $\mathbf{X}_l = \mathbf{b}_l \circ \mathbf{a}_l = \mathbf{b}_l \mathbf{a}_l^T \in \mathbb{C}^{J \times I}$ associated with the l-th column of $\mathbf{Y}$, that is, $\mathbf{y}_l = \mathbf{a}_l \diamond \mathbf{b}_l \in \mathbb{C}^{IJ}$, where $\mathbf{a}_l$ and $\mathbf{b}_l$ are the l-th columns of $\mathbf{A}$ and $\mathbf{B}$, respectively, and then calculating the SVD: $\mathbf{X}_l = \text{unvec}_{J \times I}(\mathbf{y}_l) = \mathbf{U}_l \mathbf{\Sigma}_l \mathbf{V}_l^H = \sigma_l(1) \mathbf{u}_l(1) \mathbf{v}_l^H(1)$, where $\mathbf{u}_l(1)$ and $\mathbf{v}_l(1)$ are respectively the left and right singular vectors associated with the dominant singular value $\sigma_l(1)$.

The estimates of the column vectors $\mathbf{a}_l$ and $\mathbf{b}_l$ are then given by:

$$\hat{\mathbf{a}}_l = \sqrt{\sigma_l(1)} \mathbf{v}_l^*(1) \ , \ \hat{\mathbf{b}}_l = \sqrt{\sigma_1(1)} \mathbf{u}_l(1), \tag{A.1}$$

and therefore $\hat{\mathbf{A}} = [\hat{\mathbf{a}}_1, \cdots, \hat{\mathbf{a}}_L]$ and $\hat{\mathbf{B}} = [\hat{\mathbf{b}}_1, \cdots, \hat{\mathbf{b}}_L]$.

Note that the estimates $(\hat{\mathbf{a}}_l, \hat{\mathbf{b}}_l)$ are unique up to a scalar ambiguity which can be removed using the knowledge of one component of $\mathbf{a}_l$ or $\mathbf{b}_l$.

Appendix B. Multiple KRF (MKRF) algorithm

Consider the multiple Khatri-Rao product (KRP) of M vectors $\mathbf{u}^{(m)} \in \mathbb{C}^{I_m}$:

$$\mathbf{y} = \overset{M}{\underset{m=1}{\diamond}} \mathbf{u}^{(m)} \in \mathbb{C}^{I_1 \cdots I_M}. \tag{B.1}$$

The MKRF algorithm allows to estimate the vectors $\mathbf{u}^{(m)}$ from their KRP $\mathbf{y}$. The idea behind this algorithm is to apply the KRF algorithm after some permutations of the vectors $\mathbf{u}^{(m)}$. For estimating the first and last vectors, $\mathbf{u}^{(1)}$ and $\mathbf{u}^{(M)}$, it is possible to apply directly KRF by chosing the vectors $\mathbf{a}_l$ and $\mathbf{b}_l$ as:

$$\mathbf{a}_l = \mathbf{u}^{(1)} \ , \ \mathbf{b}_l = \overset{M}{\underset{m=2}{\diamond}} \mathbf{u}^{(m)} \tag{B.2}$$

$$\mathbf{a}_l = \overset{M-1}{\underset{m=1}{\diamond}} \mathbf{u}^{(m)} \ , \ \mathbf{b}_l = \mathbf{u}^{(M)}. \tag{B.3}$$

The estimates of $\mathbf{u}^{(1)}$ and $\mathbf{u}^{(M)}$ are then provided by the KRF algorithm as the vectors $\hat{\mathbf{a}}_l$ and $\hat{\mathbf{b}}_l$ defined in (A.1), respectively. For estimating the other vectors $\mathbf{u}^{(m)}$, with $m \in \{2, \cdots, M-1\}$, we use a permutation matrix $\mathbf{\Pi}_m$ which places $\mathbf{u}^{(m)}$ at the first position in the MKRP $\mathbf{y}$, without modifying the position of the $M - m$ last vectors, which gives the following equation [36]:

$$\Big(\mathbf{\Pi}_m \otimes \mathbf{I}_{I_{m+1} \cdots I_M} \Big) \mathbf{y} = \mathbf{u}^{(m)} \overset{m-1}{\underset{j=1}{\diamond}} \mathbf{u}^{(j)} \overset{M}{\underset{j=m+1}{\diamond}} \mathbf{u}^{(j)} \tag{B.4}$$

where $\mathbf{I}_{I_{m+1}\cdots I_M}$ is the identity matrix of order $\prod_{j=m+1}^{M} I_j$, and $\mathbf{\Pi}_m$ is the permutation matrix of order $\prod_{j=1}^{m} I_j$ given by [36]:

$$\mathbf{\Pi}_m = \sum_{i_1=1}^{I_1} \cdots \sum_{i_m=1}^{I_m} \left(\mathbf{e}_{i_m}^{(I_m)} \overset{m-1}{\underset{j=1}{\otimes}} \mathbf{e}_{i_j}^{(I_j)} \right) \left(\overset{m}{\underset{j=1}{\otimes}} \mathbf{e}_{i_j}^{(I_j)} \right)^T \tag{B.5}$$

$\mathbf{e}_{i_m}^{(I_m)}$ being the i_m-th vector of the canonical basis of $\mathbb{R}^{I_m}$.

In the case of a multiple KRP of M matrices $\mathbf{S}^{(m)} \in \mathbb{C}^{I_m \times L}$, that is, $\mathbf{S} = \overset{M}{\underset{m=1}{\diamond}} \mathbf{S}^{(m)}$, the MKRF algorithm previously described for the MKRP of M vectors can be applied to each column of $\mathbf{S}$. It is important to note that this computation can be made in parallel, column by column.

Assuming the first row of each matrix $\mathbf{S}^{(m)}$ is composed of 1's, i.e., $\mathbf{S}_{1\cdot}^{(m)} = [1 \cdots 1]$, the scaling ambiguities on the estimates $\hat{\mathbf{S}}^{(m)}$ can be removed using the following equation:

$$\hat{\hat{\mathbf{S}}}^{(m)} = \hat{\mathbf{S}}^{(m)} \mathbf{\Delta}_{S^{(m)}} \text{ with } \mathbf{\Delta}_{S^{(m)}} = \left[\text{diag}(\hat{\mathbf{S}}_{1\cdot}^{(m)}) \right]^{-1}, \; m \in \langle M \rangle, \tag{B.6}$$